

Science with a small two-band UV-photometry mission II: Observations of stars and stellar systems

Jiří Krtička^{1*†}, Jan Benáček^{2,3†}, Jan Budaj^{4†}, Daniela Korčáková^{5†}, András Pál^{6†}, Martin Piecka^{7†}, Miloslav Zejda^{1†}, Volkan Bakış⁸, Miroslav Brož⁵, Hsiang-Kuang Chang⁹, Nikola Faltová¹, Rudolf Gális¹⁰, Daniel Jadlovní¹, Jan Janík¹, Jan Kára⁵, Jakub Kolář¹, Iva Krtíčková¹, Jiří Kubát¹¹, Brankica Kubátová¹¹, Petr Kurfürst¹, Matúš Labaj¹, Jaroslav Merc⁵, Zdeněk Mikulášek¹, Filip Münz¹, Ernst Paunzen¹, Michal Prišegen^{12,1}, Tahereh Ramezani¹, Tatiana Rievajová¹, Jakub Řípa¹, Linda Schmidtbreich¹³, Marek Skarka^{1,11}, Gabriel Szász¹, Werner Weiss⁷, Michal Zajaček¹ and Norbert Werner¹

¹Department of Theoretical Physics and Astrophysics, Faculty of Science, Masaryk University, Kotlářská 2, Brno, 611 37, Czech Republic.

²Institute for Physics and Astronomy, University of Potsdam, Karl-Liebknecht-Straße 24/25, Potsdam, 14476, Germany.

³Centre for Physics and Astronomy, Technical University of Berlin, Straße des 17. Juni 135, Berlin, 10623, Germany.

⁴Astronomical Institute, Slovak Academy of Sciences, Tatranská Lomnica, 05960, Slovak Republic.

⁵Astronomical Institute, Faculty of Mathematics and Physics, Charles University, V Holešovičkách 2, Praha, 180 00, Czech Republic.

⁶Research Centre for Astronomy and Earth Sciences, Konkoly Observatory, Konkoly-Thege M. út 15-17, Budapest, H-1121, Hungary.

⁷Department of Astrophysics, University of Vienna, Türkenschanzstraße 17, Vienna, 1180, Austria.

⁸Faculty of Science, Department of Space Sciences and Technologies, Akdeniz University, Antalya, 07058, Türkiye.

⁹Institute of Astronomy, National Tsing Hua University, 101 Sec. 2 Kuang-Fu Rd., Hsinchu, 300044, Taiwan, Republic of China.

¹⁰Institute of Physics, Faculty of Science, P. J. Šafárik University, Park Angelinum 9, Košice, 040 01, Slovak Republic.

¹¹Astronomical Institute, Czech Academy of Sciences, Fričova 298, Ondřejov, 251 65, Czech Republic.

¹²Advanced Technologies Research Institute, Faculty of Materials Science and Technology in Trnava, Slovak University of Technology in Bratislava, Bottova 25, Trnava, 917 24, Slovakia.

¹³European Southern Observatory (ESO), Alonso de Cordova 3107, Vitacura, Santiago, Chile.

*Corresponding author(s). E-mail(s): krticka@physics.muni.cz;

†These authors contributed equally to this work.

Abstract

We outline the impact of a small two-band UV-photometry satellite mission on the field of stellar physics, magnetospheres of stars, binaries, stellar clusters, interstellar matter, and exoplanets. On specific examples of different types of stars and stellar systems, we discuss particular requirements for such a satellite mission in terms of specific mission parameters such as bandpass, precision, cadence, and mission duration. We show that such a mission may provide crucial data not only for hot stars that emit most of their light in UV, but also for cool stars, where UV traces their activity. This is important, for instance, for exoplanetary studies, because the level of stellar activity influences habitability. While the main asset of the two-band UV mission rests in time-domain astronomy, an example of open clusters proves that such a mission would be important also for the study of stellar populations. Properties of the interstellar dust are best explored when combining optical and IR information with observations in UV. It is well known that dust absorbs UV radiation efficiently. Consequently, we outline how such a UV mission can be used to detect eclipses of sufficiently hot stars by various dusty objects and study disks, rings, clouds, disintegrating exoplanets or exoasteroids. Furthermore, UV radiation can be used to study the cooling of neutron stars providing information about the extreme states of matter in the interiors of neutron stars and used for mapping heated spots on their surfaces.

Keywords: techniques: photometric, ultraviolet: stars, stars: variables: general, binaries: general, open clusters and associations: general, planetary systems

1 Introduction

The new discoveries in astrophysics during the last few decades were frequently connected with the opening of new observational windows into invisible parts of the spectrum. Recently, the advent of observatories working outside the electromagnetic domain founded a new branch of science called multimessenger astronomy. From this, it may seem that new observations in the most classical domain of astronomy, the optical domain, can hardly revolutionize the field of astrophysics. And yet, small and medium-sized satellite missions such as *CoRoT* (Auvergne et al. 2009), *Kepler* (Borucki et al. 2010), *MOST* (Walker et al. 2003), *BRITe* (Weiss et al. 2014), and *TESS* (Ricker et al. 2015) opened a new window into time-domain astronomy, extending far beyond the physics of variable stars and exoplanetary systems.

Similar advances may be expected from photometric missions working in other domains of the electromagnetic spectrum. In this paper, we outline the impact of a small two-band ultraviolet (UV) photometric satellite mission on the field of stars, binaries, stellar clusters, interstellar matter, and exoplanets. The paper is based on QUVIK – Quick Ultra VIolet Kilonova surveyor (Werner et al. 2024, hereafter Paper I), an approved Czech national science-technology mission. QUVIK is a small 130 kg satellite that will be launched to a low-Earth, Sun-synchronous, dawn-dusk orbit at the end of this decade. Its telescope will have a moderately large field of view of about $1.0^\circ \times 1.0^\circ$ and two UV bands. The far-UV band is planned to have a bandwidth of approximately 140–180 nm, and the near-UV band will span 260–360 nm. The primary objective of QUVIK is the study of electromagnetic counterparts of gravitational wave sources, such as kilonovae (Paper I). Besides stellar astrophysics, the proposed science includes the study of galactic nuclei and nuclear transients described in Paper III of the series (Zajaček et al. 2023).

QUVIK will provide absolutely calibrated data. This requires calibration on the ground before the launch and onboard during the flight. The pre-flight ground calibration procedures include spectral measurements of the throughput of the individual parts of the optical system. The spectral response and zero point will be determined by observing standard photometric sources such as individual stars, white dwarfs, and open clusters.

2 Physics of Stars

The most important characteristic that describes the observational appearance of stars is their effective temperature because it mostly determines the stellar spectral energy distribution. Therefore, the effective temperature tells us what we can learn from observations of stars in different spectral domains. According to their effective temperature, stars are conventionally divided into two large groups: cool stars and hot stars. While hot stars (with effective temperatures higher than about 7000 K) emit most of their light in UV, and therefore UV enables us to understand the physics of these stars, cool stars emit only a small part of their flux in the UV domain, most notably from outer layers of

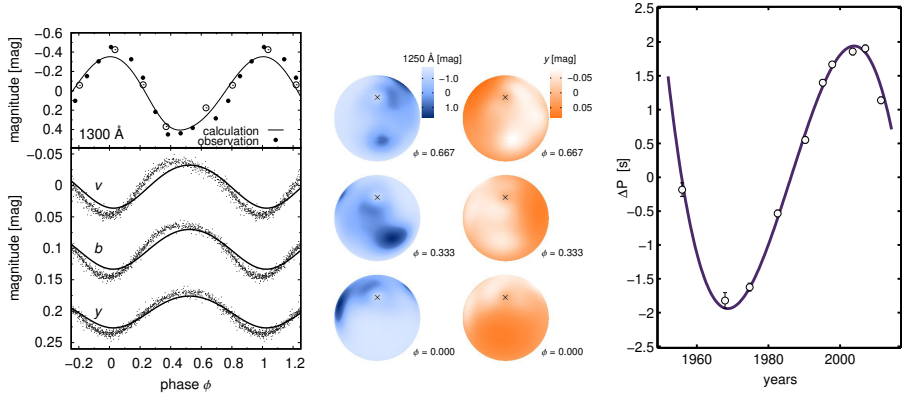


Fig. 1 Variability of chemically peculiar CU Vir. *Left:* The light curve in ultraviolet (upper panel) and visual (lower panel – Strömgren *vby* filters) domains. Empty circles denote HST observations (Krtićka et al. 2019). *Middle:* The emergent intensity at various rotational phases ϕ in the ultraviolet (blue plots) and visual (orange plots) domains. *Right:* Rotational period variations with respect to the mean period derived from photometry (Mikulášek et al. 2011).

their atmospheres called chromospheres (Ayres et al. 1981). Consequently, in cool stars, the UV tells us a lot about their activity and their impact on the surrounding environment.

Although our knowledge of stars has advanced enormously during the last century, many questions related to the evolution of stars and their impact on the surrounding environment remain unanswered. This has a strong impact on other fields of astrophysics, including the physics of binary compact star merger sources of gravitational waves or the study of the interaction of stars and their exoplanets. Surprisingly, even a small-size UV satellite can help to solve many of these open questions. In the following, we explain how.

2.1 Tests of opacities

Opacities are one of the key ingredients of any numerical stellar model. Therefore, any uncertainty in opacity has a strong influence on the reliability of stellar models. For instance, inaccurate opacities are one of the suspects of the difference between the sound speed determined for our Sun from helioseismology and the sound speed derived from solar models (Basu 2018). Incorrect opacities due to rare-earth elements may cause the mismatch between the predicted and observed light curves of kilonovae (Wu et al. 2022). The inclusion of iron peak opacities into models provides a textbook example of the importance of opacities for triggering pulsations (Iglesias et al. 1992).

Therefore, opacity calculations are of enormous value, and the measurement of opacities belongs to very important tasks for laboratory astrophysics. However, testing opacities for actual stellar conditions would be even more valuable. Here comes the hardly replaceable role of chemically peculiar stars.

These hot stars show patches with peculiar abundances of different elements on their surfaces (Kochukhov & Ryabchikova 2018, see Fig. 1), resulting from a complex interplay between radiative and gravitational acceleration (e.g., Michaud et al. 2011). Chemically peculiar stars show rotationally modulated light variability, caused by horizontal variations of opacity in surface patches, which redistribute flux mostly from far-UV to near-UV and visual domains (Peterson 1970; Lanz et al. 1996). A comparison of predicted and observed light curves enables us to test the opacities involved in the modelling of the outer layers of these stars (Prvák et al. 2015; Krτίčka et al. 2019, Fig. 1). Cool chemically peculiar stars are of special interest, because in these stars the opacities of rare-earth elements are supposed to play a decisive role.

Because most well-studied chemically peculiar stars are relatively bright, it is recommended that the telescope should enable to observe also stars with magnitude of at least 4 mag or even brighter. The typical rotational period of these stars is on the order of days; therefore, to sufficiently cover the light curve of these stars, the highest required cadence is 15 min for stars with the shortest rotation period of about half of a day. The study would benefit from observations in the UV, where the variability is the strongest and where antiphase behaviour of the light curves (with respect to the optical domain) is expected. From optical amplitudes of up to 0.1 mag, the required signal-to-noise ratio (SNR) of individual photometric data is about 100. For a reliable comparison with theoretical light curves, detailed knowledge of the instrumental response function is needed.

A far-UV band enables to trace opacities due to silicon and iron, which have a maximum in this region (Prvák et al. 2015). Moreover, this band is ideal for studying hot chemically peculiar stars, in which the flux variability originates in the far-UV region.

2.2 Probing the surface structure in normal B and A-type stars

High-precision satellite photometry of normal main-sequence B and A-type stars revealed an unexpected phenomenon: a plethora of weak surface spots (Balona 2011, 2017). This discovery came as a complete surprise as hot stars lack deep subsurface convective zones. As a result, a revision of the physics of stellar envelopes comprising cool spots has been suggested (Balona 2017). A more conservative approach advocates a general model of a surface consisting of overabundant spots, irrespective of the peculiar nature of the stars (Krτίčka et al. 2014).

UV photometry can provide an answer about the structure of the stellar surface in normal B and A-type stars. Signatures of abundance spots in a spectral energy distribution differ from those of temperature spots. Consequently, precise observation in two bands should provide data that can be tested against models, including abundance and temperature spots.

This task requires observations with an SNR of 1000 (of individual photometric measurements) to detect the variability (Balona 2011). Based on

available optical light curves, a higher cadence of observations of 5 min is needed to obtain well-sampled light curves. The test requires observations in a far-UV and near-UV bands to get simultaneous observations in two bands. This combination would reliably distinguish between the two models because the expected amplitude of variability is larger in the far-UV band.

2.3 Understanding the cyclical chromospheric activity and its evolutionary changes in cool stars

Dynamo action powered by convection and differential rotation in envelopes of cool stars gives rise to variable surface magnetic fields and activity (Chatterjee et al. 2004). A strong magnetic field suppresses convective energy transport in localized surface regions, leading to the formation of cool surface spots, which appear dark due to their lower effective temperature (e.g. Granzer et al. 2000). On top of that, part of the energy flux transported by subsurface convective motions heats the chromospheres and coronae of cool stars. Except for variations due to flares, the UV flux shows rotational variations (Hallam & Wolff 1981), variations during the activity cycle as measured in our Sun using the *SORCE* satellite (Harder et al. 2009), and variability in the course of the stellar lifetime (Guinan & Engle 2007).

The evolutionary variability of the UV flux, that is, change of both mean flux and the properties of short-term variations, can be determined from observations of individual cool stars with different masses and ages. This can tell us if the UV chromospheric flux varies with age in a similar way to X-ray activity or rotation (Ribas et al. 2005). Such a study requires observations below 285 nm, where the chromosphere contribution dominates (Ayres et al. 1981; Stencel et al. 1986; Johnson & Luttermoser 1987). Therefore, far-UV band of *QUVIK* could be used to probe the chromosphere, while the near-UV band would be contaminated by photospheric flux. Alternatively, simultaneous UV observations in the 220–290 nm band with *ULTRASAT* (Shvartzvald et al. 2023) would provide a complementary probe of the chromosphere. The far-UV band is also important for the interaction of cool stars with their exoplanets (see Sect. 6.2). The expected evolutionary variability is relatively large, therefore, a medium SNR of about 100 is required.

Besides the evolutionary variability, cyclical variability of chromospheric emission may also have an impact on planetary atmospheres on the timescale of several orbits. While the basic period of solar activity is typically too long to be detected by a single small satellite, other stars show shorter periods of activity of a few years (Wilson 1978; Baliunas et al. 1995). Such a periodicity can be detected even by a mission with a duration shorter than the solar cycle. As a result of similar amplitude of flux changes, the requirements of such observations are basically the same as for the study of evolutionary changes, except for cadence, which is required of about 14 days due to an expected order-of-year-long period of this type of variability.

The flaring activity of our Sun became proverbial. However, flares are more typical in stars much cooler than the Sun, in M dwarfs, where the star may

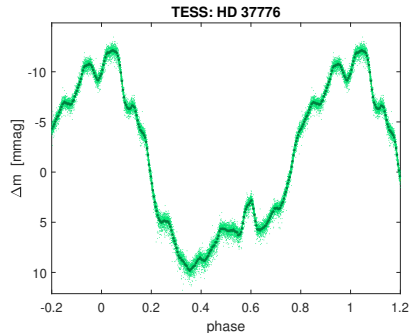


Fig. 2 TESS light curve of a chemically peculiar star HD 37776. Besides the large-amplitude rotational variability (due to horizontal opacity variations), the light curve shows regular short-term variability dubbed ‘warps’ by Mikulášek et al. (2020).

brighten by several orders of magnitude (Froning et al. 2019). Flares are the aftermaths of a sudden release of magnetic energy that affects the stellar surface (Haisch et al. 1991). This locally heats the atmospheres to temperatures of the order of tens of thousand kelvins and leads to a brightening of a star (Allred et al. 2006). Due to the high temperature of flaring matter, flares can be best studied in the ultraviolet domain (Doyle et al. 1989; Welsh et al. 2006). The study of UV light curves of flaring stars can help to understand the properties of flares (Froning et al. 2019), their frequency, and their influence on surrounding exoplanets. To fit the light curves of flares and to determine flare properties (Kowalski & Allred 2018), observations in both far-UV and near-UV bands are required. Because the flares can appear on a timescale of seconds and their occurrence cannot be predicted, monitoring of a given star for days with a cadence of 1 s is needed to determine the flaring activity. A medium SNR of 100 is sufficient for this purpose.

2.4 Nature of warps in the light curves of magnetic stars

High-precision satellite observations of chemically peculiar stars revealed multiple persistent phase-locked warps on their light curves (Mikulášek et al. 2020, see Fig. 2). The warps likely originate due to the light absorption in centrifugally supported magnetospheric clouds reminiscent of stellar prominences (Krtićka et al. 2022). The clouds are expected to be fed by wind, providing the only evidence of winds in low-luminosity hot stars. However, the competing model predicting the other origin of the warps due to surface features was not yet excluded. High-precision observations in two bands can resolve the issue. Magnetospheric absorption originates on free electrons; therefore, it is predicted to be grey. On the other hand, variability due to surface features is expected to show different amplitudes in different bands. Therefore, precise photometric observations in two filters will allow us to understand the nature of warps in the light curves of chemically peculiar stars and possibly prove the existence of stellar wind. Observations with a relatively high SNR of 1000 are

required to clearly determine the amplitude of the warps (see Fig. 2). The corresponding cadence of observations should be about 1 min to observe warps with high time resolution. The near-UV band combined with optical photometry is suitable to distinguish between the models of variability. Alternatively, a far-UV band would enable an even better test of the nature of light absorption in hot stars with corotating magnetospheres (Oksala et al. 2015) and extremely hot white dwarfs (Reindl et al. 2019).

2.5 Determining the drivers of line-driven wind instability

Photometers on board satellite missions detected low-amplitude light variations of single O-type stars. These variations were attributed to gravity waves (Aerts et al. 2017) or subsurface convection (Blomme et al. 2011). However, there is an intriguing possibility that this variability bears the signature of a line-driven wind instability (deshadowing instability, Krτίčka & Feldmeier 2018). This would imply that we are able to detect seeds of line-driven wind instability in photometry. Understanding and detailed modelling of this instability are crucial for deriving the precise wind mass-loss rate of hot stars from observations (e.g. Sundqvist et al. 2010; Šurlan et al. 2013).

Continuous photometric observation of selected stars in two bands is needed to distinguish between individual sources of stochastic light variability. Wind blanketing and changes of temperature affect atmospheres in different ways. Therefore, the amplitudes and signatures of the variability in two bands provide the key observables in this case (Krτίčka & Feldmeier 2018). This requires continuous photometry for several days. A relatively high SNR of 1000 and cadence of about 30 s is needed to clearly detect the variability. A reasonable option is to use a near-UV band in combination with a far-UV band, where the light variability due to wind blanketing is strong (Krτίčka & Feldmeier 2018).

2.6 Unveiling the mass-loss histories of Be and B[e] stars

Massive stars are born with masses higher than about $8 M_{\odot}$, but leave a compact remnant with a typical mass of a few solar masses. When did the mass get lost? We are not sure (Smith 2014), and that is why we have to explore different evolutionary stages to understand when mass loss happens. B[e] stars and most notably B[e] supergiants belong to the evolutionary stage during which a significant amount of mass can be lost. Long-term UV observations of these stars can distinguish between individual states of the envelope caused by, e.g., variable disk absorption or LBV-type variations (Hutsemekers 1985; Shore 1990; Krτίčková & Krτίčka 2018). Furthermore, UV variability provides information on the structure of the envelope in Be stars (Smith 2001). Observations in two UV bands revealed that some B[e] stars maintain constant luminosity during their photometric variations, providing a better understanding of the drivers behind the variability (Krτίčková & Krτίčka 2018). The study also showed that

the UV band is ideal for detecting pulsations, enabling us to understand the mechanism behind the outbursts in these stars.

A typical timescale of the variability of B[e] star circumstellar environment is of the order of months; therefore, a cadence of observations of 14 days should be sufficient. The variability shows relatively large amplitudes, which translates into a loose constraint on SNR of about 10. The study requires observations in the near-UV band, where the variability due to variable effective temperature and dust obscuration is strong. The analysis would benefit from simultaneous UV observations in the 220–290 nm band with *ULTRASAT*, whose band is located close to the carbon opacity bump. The inclusion of a far-UV band would enable the construction of near reddening-free colour-magnitude diagrams (Krtičková & Krtička 2018), which probe luminosity variations.

Be stars display variability on various time scales. Usually, this variability is described as long-term (years), medium-term (days to tens of days), and short-term (fraction of a day). This variability is caused by different mechanisms, such as disk growth and dissipation or disk waves (Rivinius et al. 2013) and pulsations (e.g., Baade et al. 2016) and is visible in spectral line profiles and photometry. There exist observational records of visual photometric observations of Be stars (e.g. Pavlovski et al. 1997, Labadie-Bartz et al. 2017). Simultaneous observations in visual and far-UV or near-UV bands would significantly help to understand the Be star variability. The observational effort may include all variability time scales, from short to long. The required cadence depends on the properties of the objects.

2.7 Mass-loss mechanism in cool supergiants

After decades of studies, the wind mechanism in cool supergiants is still not very well understood. Processes invoked to explain cool supergiant outflows include the radiation force on dust grains, pulsations, and convection. Humphreys & Jones (2022) suggested that most of the mass-loss in these stars is connected with episodic gaseous outflows similar to that linked to the Great Dimming of archetypal cool supergiant Betelgeuse (see also Sect. 7). This can be tested using UV observations. The proposed mechanism for this dimming, which includes dust cloud (Levesque & Massey 2020; Montargès et al. 2021) and changes in stellar effective temperature (Dharmawardena et al. 2020), has to cope with the near constant brightness of the star in the infrared (Gehrz et al. 2020). Variable dust absorption and changing effective temperature can be distinguished, especially at short wavelengths, due to the different dependence of amplitudes on wavelength (Jadlovský et al. 2023).

A typical time delay between ejections of individual clumps of the order of years (Humphreys et al. 2021) is comparable to the duration of a small mission. Therefore, the frequency of episodic gaseous outflow events in cool supergiants should be estimated from the observation of a sample of these stars in two UV bands, including the near-UV band and either far-UV or optical band. Given the long timescale of the variability of these stars, the 1-day cadence should be sufficient with the required SNR ratio of about 100.

2.8 Understanding pulsating stars of the upper main sequence

Pulsating stars allow one to probe stellar interiors, which are not accessible to direct observations. Therefore, the physical conditions and processes within a star can only be observed through their influence on the pulsation periods and amplitudes. Pulsations provide an elegant way to derive stars' basic fundamental properties, such as mass, radius, and distance (De Ridder et al. 2009; Bedding et al. 2011; Belkacem et al. 2011; Miglio et al. 2013).

Several different types of pulsating stars appear in the upper main-sequence region of the Hertzsprung–Russell diagram. They include β Cephei stars, which are very massive p-mode (pressure mode) pulsators (Salmon et al. 2022), δ Scuti stars, which are multiperiodic pulsating variables located in the lower part of the Cepheid instability strip, and rapidly oscillating Ap stars (Kurtz 1990), which belong to chemically peculiar stars with pulsational variability in the period range of 5 to 25 minutes. Pulsating stars of the upper main sequence include also g-mode (gravity mode) pulsators, such as slowly pulsating B-type stars, which pulsate in high-order modes (Christophe et al. 2018), and γ Doradus stars, which are intermediate-mass, late-A/early-F stars, located at the cool border of the classical δ Scuti instability strip, pulsating in high-order g-modes (Guzik et al. 2000).

If we look at any models describing these classes of variable stars, we find that the amplitudes typically increase significantly with decreasing wavelength (Guzik & Roth 2021). The increase is strongly dependent on the rotation (especially of the core), the metallicity, and mass-loss rate. However, in the UV we have so far only sparse information from ground-based observations in Johnson *U*, for example. Time-series in the UV are, therefore, very much needed to test and calibrate our current pulsational models. This will be an excellent supplement to the data from the *Kepler*, *PLATO*, and *TESS* missions.

To advance the physics of stellar pulsations, simultaneous (or near-simultaneous within minutes) observations in two bands are required. Both bands should be preferably located in UV to obtain a larger amplitude of variability. The benefits of two-color photometry are illustrated, e.g., by Weiss et al. (2021). Individual pulsating stars show very different periods; therefore, depending on the variability type, the required cadency is from 5 minutes up to days. For the pulsational analysis, a high SNR of about 1000 is needed.

2.9 Neutron stars

Neutron stars (NS) are strongly magnetised (10^8 – 10^{13} G), high-density (10^6 – 10^{14} g cm⁻³) fast-rotating objects with periods from milliseconds to several hundred seconds. They are unique laboratories to study degenerate matter inside peculiar objects (Lorimer & Kramer 2004). In addition, there are also specific types of NSs that manifest further kinds of accompanying physical effects – pulsars, accretion-powered NSs, interacting NSs in binaries, merging NSs, and magnetars (a type of NS with an extremely strong magnetic field).

Magnetars might be related to the recently discovered phenomenon of fast radio bursts (FRBs), mysterious millisecond transients currently only detected at radio frequencies whose nature is still unclear (CHIME/FRB Collaboration 2020; Xiao et al. 2021; Petroff et al. 2022), see Paper I.

There is still a lot of uncertainty about the evolution of NSs, their internal structure and the structure of their magnetospheres, the sources of their UV emission, locations of these emission regions, and whether there is, and to what degree, a relation between magnetars and FRBs. UV observations are crucial to resolve these questions, but are very scarce to date and could be relatively easily provided by a small satellite.

2.9.1 Revealing the internal composition of neutron stars by studying their thermal evolution

NSs cool down via photon and neutrino emissions at timescales of tens of millions of years. This evolution provides an important way to reveal NS composition, properties, and equation of state. If an NS cools only passively, its effective temperature is expected to drop below 10^4 K in ~ 10 Myr. However, various heating processes slow down (and in some cases even reverse) the cooling (Gonzalez & Reisenegger 2010). For old NSs, the measured effective temperatures have been shown to be significantly higher than predicted by cooling models (Abramkin et al. 2022). There are models of heating processes such as rotochemical heating and heating due to magnetic field decay. Moreover, NSs were proposed to attract dark matter because of their high mass. As dark matter reaches the interior of the NS, its interactions with neutron matter might lead to a measurable heating of the star (Köpp et al. 2023).

Because the maximum thermal emission of NSs is in the UV range due to their high effective temperatures, these processes are difficult to be observed from the ground. To properly estimate the spectral index in the UV, observations should be made in at least two filters. Additional spectral points necessary to fit black-body radiation can be obtained from observations at visible and X-ray wavelengths from archives.

A specific objective for the small satellite can be to estimate the effective surface temperature of five to ten middle-aged to old NSs. By observing in two UV filters, quantitative estimates of the NS surface temperature can be obtained and compared with the temperature from NS evolution models. Constraints on the NS effective temperatures would allow refinements of the evolution models and constrain the internal structure, composition of NSs, and NS heating process(es). Since old NSs are stable on long timescales, observations are not time critical and can be obtained at any time during the mission.

We identified seventeen candidate pulsars with expected magnitudes brighter than 22 mag in the UV range (Høg et al. 2000; Hobbs et al. 2004; Mignani 2011; Gaia Collaboration 2020). All have been found at least at visual and radio wavelengths simultaneously. If no UV data were available, we estimated their brightness to be 2 magnitudes fainter than the V-band magnitude,

based on the typical intensity difference of the known pulsars. Also, this difference is consistent with old NSs that have been simultaneously observed in the visual and UV range. Some of the candidates are already covered in UV (Abramkin et al. 2022); however, these measurements are not suited to estimate spectral indices, for which we would need observations made in two UV filters. For a NS magnitude of 22 mag, expected as a practical limit by QUVIK, we get $\text{SNR} \sim 23$ in ~ 20 hours, which is sufficient for the proposed estimations of the spectral slope of the black-body radiation.

2.9.2 Mapping the emission regions on the neutron star surface

At the surface of the NS, heated regions can be formed, which have been observed in soft X-rays (Guillot et al. 2019). These are magnetic pole regions where relativistic particles (the so-called returned current) from the magnetosphere can hit and heat these spots. During the rotation of the NS, the measured flux changes due to the movement of these heated regions, allowing it to constrain the impact of individual regions. However, the observed UV radiation may originate from these regions (hot spots) with a thermal nature or from other locations in the NS magnetosphere with a non-thermal nature, or a combination of them. For the magnetospheric origin, the emission mechanisms and locations remain unclear. More recent models for the non-thermal emission from pulsars include, for example, the striped-wind model (Pétri 2015), the extended-slot-gap and equatorial-current-sheet model (Barnard et al. 2022), the synchro-curvature model (Íñiguez-Pascual et al. 2022), and the non-stationary outer-gap model (Takata & Cheng 2017). UV observations to disentangle the thermal and non-thermal components can help to constrain theoretical models. Moreover, the emission mechanisms and regions of magnetars are very likely different from those of other classical neutron stars. If the heated surface regions are located where the magnetic field penetrates the star, monitoring of the emission regions allows refining the long-standing and highly-discussed issue between a dipolar (classical NS) or multipolar (magnetars) shape of the magnetosphere, the relation between the different magnetosphere shapes and their impact on the NS evolution (Yao et al. 2018).

UV photometry can provide an important way to model the thermal spots and shape of the magnetosphere. To characterise the location of their emission regions, the aim can be to determine the UV light curves for pulsars (periods < 1 s) and magnetars (periods ~ 10 s) in the near- and far-UV filters, compare the light curves with those observed in X-rays and visual range and localise the emission regions based on inverse modelling (Riley et al. 2019).

The candidate objects have $\lesssim 16$ mag for pulsars and $\lesssim 18$ mag for magnetars in the UV range. Each measurement should be long enough to obtain $\text{SNR} \sim 70$ for pulsars and $\text{SNR} \sim 45$ for magnetars. The exposure time can be divided into sub-exposures, each of them set to $\sim 1/15$ – $1/30$ of the NS rotation period (typically 1 ms–1 s). The sub-exposures have to be aggregated according to the NS rotation phase to obtain the average phase curve. This

short-time observing mode would be unique for the UV observations of a small satellite and can only be provided by a very few instruments. The observations can be obtained over the whole mission in more time intervals, given that the precision of the sub-exposure time stamp is significantly higher than the exposure time itself. Furthermore, as some of the NSs show sudden changes in their rotation phase (called glitches), their measurements have to be done in a time interval of a day or a few days. The fast read-out window of the chip has to be scalable and large enough to include the whole PSF of the stars. Similarly, the exposure time has to be changeable down to a few milliseconds.

3 Binary stars

A substantial fraction of stars are found in binary or multiple stellar systems. The binary star fraction depends on the stars' spectral types (Moe & Di Stefano 2017). Most massive and luminous stars appear typically in binaries or triple systems; on the other hand, red dwarfs spend their lives mostly alone. Binary stars are crucial in astrophysical research because they are unique sources of information. Their orbits provide the most important stellar parameter, the masses of stars. The most precise and direct determinations of masses are enabled using visual or eclipsing binaries which are also spectroscopic binaries (Serenelli et al. 2021). The values of masses at an accuracy better than 1–3% are necessary for tests of models of stellar evolution (Andersen 1991; Torres et al. 2010). Binary stars provide an extremely large amount of data about stars, their atmospheres, stellar winds, plasma physics, and the interaction between stars and their surroundings. They can be used for an independent distance determination (Southworth et al. 2005; Graczyk et al. 2021).

The world of binaries is very diverse. In detached pairs in relatively wide orbits, the companions evolve almost independently, allowing us to accurately determine the component masses, radii, and temperatures. By taking into account their age and chemical compositions, we can use them to constrain and calibrate models of stellar evolution. Such systems were used to study the primordial helium abundance, the helium-to-metals enrichment ratio (Paczynski & Sienkiewicz 1984; Brogaard et al. 2012), the convective core overshooting, the mixing length parameter (Guinan et al. 2000; Claret & Torres 2018), mass loss by stellar winds (Ignace et al. 2022), and standard luminosities and multi-band bolometric corrections (Bakış & Eker 2022). If the stars in a binary system are close enough to fill their Roche lobes, we speak about semi-detached or contact binary. In such close binaries, mass exchange between companions or mass loss from the system occurs during their lifetime. Many different phenomena can then be studied: tidal effects, mass transfer, mass loss, and orbital angular momentum loss (e.g. Loukaidou et al. 2022). When the mass transfer occurs during the supergiant evolutionary phase of the more massive component, the star is stripped off its envelope. Consequently, the evolution may lead to objects such as cataclysmic variables, X-ray binaries, (super-, hyper-, kilo-)novae, millisecond pulsars, double-degenerate systems, and generation

of short gamma-ray bursts or gravitational waves (Podsiadlowski et al. 2002; Antoniadis et al. 2013).

3.1 Galactic and extragalactic massive binaries

The origin and further evolution of massive binaries are still not fully understood. However, these binaries are of special interest, because the final stage of their evolution results in very bright transient events caused by super-, hyper-, kilonovae, or mergers generating gravitational waves. To evaluate and improve the models of stellar evolution, we need to know the masses and radii of stars. The easiest way to obtain these parameters is to study eclipsing double-lined spectroscopic binaries. There are more than two million known eclipsing binaries (Gaia Collaboration et al. 2021). However, only less than 300 have the fundamental parameters determined with accuracy in 1–3% as requested for the test of stellar models (see DebCat catalogue in Southworth 2015) and only about one-fourth of the included systems have massive components (over $3 M_{\odot}$). Thus, new precise measurements in the bands, where the hot massive stars radiate predominantly, are highly demanding. Observations in UV and visible bands help to determine the radii of binary components. Two-channel observations in UV could increase the accuracy of determination of the effective temperature ratio and allow us to model the reflection effect (Pigulski et al. 2019).

To provide precise binary parameters, accurate observations in two band-passes with a time resolution of less than 5 minutes covering the whole phased light curve of selected systems are required. A combination of near-UV and the optical band could be used, but near-UV and far-UV provide better constraints for the binary system model.

3.2 (Post-)common envelope binaries

During their lives, a large number of binaries undergo a phase in which both stars share one common envelope. Such evolutionary phase and resulting post-common-envelope binaries (PCEBs) are predecessors to many extraordinary objects such as SN Ia supernovae, X-ray binaries, double degenerated binaries and others (Paczynski 1976; Wang & Han 2012; Ivanova et al. 2013).

Nowadays, surveys provide valuable data for searching PCEBs. The number of such systems containing late-type stars has increased rapidly. However, white dwarfs in PCEBs with the early-type component are outshined by their companions. The radiation of white dwarfs only makes up 1% of the total radiation of binary. However, the use of a combination of far-UV, near-UV, and optical data facilitates the detection of these PCEBs. A convenient way to detect such systems is to search for main-sequence stars with substantial UV excess as a result of the presence of a nearby white dwarf companion. This will allow us to determine the occurrence rate of PCEBs with early-type components and search for this kind of progenitors of exploding stars or mergers.

This program could be executed as complementary and use observations of binaries that, by coincidence, appear in field of view (FoV) while monitoring other primary targets.

3.3 Symbiotic binaries

Symbiotic variables are strongly interacting binary systems consisting of a cool evolved star (typically M or K giant) and a hot component (white dwarf or neutron star). These objects are unique astrophysical laboratories in the study of stellar evolution, mass transfer, accretion processes, stellar winds, jets, dust formation, or thermonuclear outbursts (e.g. [Mikołajewska 2012](#); [Munari 2019](#)).

The symbiotic stars are divided into two categories: so-called shell-burning symbiotic binaries with hydrogen burning ongoing on the surface of the white dwarf and accreting-only symbiotic stars powered by accretion. The latter group is less represented in the catalogues of symbiotic binaries (e.g. [Belczyński et al. 2000](#); [Merc et al. 2019](#); [Akras et al. 2019](#)) as the optical spectra of these symbiotic stars are often inconspicuous. They can be detected due to UV excesses, significant flickering (which is most prominent in near-UV), or their X-ray emission (e.g. [Luna et al. 2013](#); [Mukai et al. 2016](#); [Munari et al. 2021](#); [Merc et al. 2023](#)).

UV photometric mission can search for new symbiotic binaries via detection of the UV excess of the red giant branch and AGB stars. UV photometry can also be used for verification of the symbiotic candidates by searching for UV excess and/or UV flickering of the candidates. Such studies require just one UV band and 30–60 minutes time-series of short exposures of a few tens of seconds to search for flickering. Time series of UV observations can also help to study the process of accretion in symbiotic stars and in probing the physical mechanisms of the classical symbiotic outbursts, which is still debated ([Munari 2019](#)). In this case, UV observations of symbiotic stars performed in two bands supplemented with ground- and space-based optical data can put constraints on the physical mechanisms of the outbursts. Together with optical and infrared (IR) spectral energy distribution, photometry in two UV bands can also be used to improve parameters of the hot components of known symbiotic binaries. Long-term light curves (2–3 years) in one UV band sampled with a cadence of a few weeks can provide the orbital periods of symbiotic binaries on the basis of the reflection effect, which has the highest amplitude in near-UV.

3.4 Cataclysmic variable stars

Cataclysmic variables (CVs) are close, interacting binary systems comprising a white dwarf (WD) receiving mass from a Roche lobe-filling late-type star. The actual accretion process is determined by the absence or strength of the WD's magnetic field. For non-magnetic CVs, an accretion disc forms around the WD, which helps to remove the angular momentum of the in-falling material. The gas flows and connected processes in CVs are very complex. The WD and

the accretion disk reach temperatures up to 10^4 – 10^5 K; thus, their behaviour is observable best in UV. In fact, the total luminosity of an accreting CV is dominated by the luminosity of the accretion disk, which can be derived from the absolute UV magnitudes (Selvelli & Gilmozzi 2013).

The evolution of a CV is driven by the loss of angular momentum. This process controls the change of the orbital period and, in the phases of interaction, the mass transfer rate. For systems above the period gap, magnetic braking dominates the angular momentum loss, while for systems below the gap, gravitational radiation is the main contributor (for a summary, see Knigge et al. 2011). The total luminosity gives the momentary accretion rate; for dwarf novae, differences are observed between quiescent states (no accretion) and outbursts when the material from the disc is dumped onto the white dwarf. One of the key questions that can be addressed by a UV photometry mission is how the momentary mass-loss rates determined from the total luminosity compare to the secular accretion rates as revealed by WD temperature or secondary bloating. Time-domain UV observations could also help to probe the variations of the accretion rate with the orbital period. This can provide tests of theoretical models of angular momentum loss.

Comparison of these accretion rates with standard models shows that there is a possible increase in the accretion rate in the orbital period range of 3–4 h, i.e., just above the period gap. This is the domain of SW Sex stars, an evolutionary state that CVs seem to go through before they enter the period gap (Schmidtobreick 2013). While the SW Sex phenomena can be explained by assuming high accretion rates, actual values for the accretion rate have only been estimated for three of these objects (Pala et al. 2017, and references herein). Measuring the accretion rate from the UV luminosity and comparing it for SW Sex stars, classical nova-like stars, and dwarf novae will help to understand these extreme objects.

Classical novae are CVs that have been observed to have a nova eruption. Theory predicts that the WD is heated by the eruption. Subsequently, it can irradiate the secondary and thus influence the accretion rate. This would result in a change in luminosity. Selvelli & Gilmozzi (2013) compared the luminosity and spectral energy distributions of several novae at different epochs using data from various UV satellites. For most systems, they did not find a significant change over the time of ten to twenty years. A comparison with new data taken few decades later would indicate if any variation in the luminosity of the accretion disc is present on larger time scales.

For the studied dwarf novae, the analysis requires to measure the brightness during several outbursts. This will enable to determine the total luminosity and accretion rate for each measurement; from this, the overall accretion during a cycle can be established and then calculated into an average accretion rate for the system. For nova-like stars (normal ones and SW Sex type) and old novae, snapshot observations in two UV bands and are sufficient as the accretion discs are stable, and the average accretion rate can be derived directly.

3.5 RS CVn-type stars

RS CVn-type stars are variable stars found in detached binary systems. They are composed of main-sequence stars with spectral types around G–K. [Fekel et al. \(1986\)](#) gave three properties required to become a member of this group of variable stars: at least one star must exhibit emission in the H and K resonance lines of Ca II, which are created in the chromospheres of stars, systems must show light variations caused by effects other than eclipses, pulsations, or ellipticity. The more active star must be evolved, and it also has to have spectral type F, G, or K.

Brightness variations of RS CVn-type systems are caused by the large stellar spots. Typical brightness fluctuation is around 0.2 mag. The spots are created by high chromospheric activity, similar to the Sun. Some RS CVn-type systems exhibit brightness variations due to stellar eclipses superimposed on changes caused by the variation in the spot surface coverage fraction, e.g. RT And, XY UMa ([Pribulla et al. 2000, 2001](#)). Photometric variability is often correlated with chromospheric line emissions. UV emission is, by solar analogy, known to be associated with stellar active and transition regions (Sect. 2.3). These areas on the Sun are associated with intense magnetic fields, and sunspot activity is enhanced in and around these magnetically active regions. Such magnetic activity is also detected in RS CVn-type systems. [Montesinos \(1998\)](#), using combined optical and UV observations, showed a spatial correlation between photospheric spots and chromospheric plages.

Therefore, photometric observations with a UV satellite could enable studying evolution of energy loops and magnetic activity, their impact on the formation of active regions, and stellar spots. Such analysis requires multi-band observations of the whole-phased light curves of selected objects with a time resolution of up to 10 minutes.

3.6 Reflection effect in binary systems

Reflection effect is crucial in close binaries with extreme temperature differences between the components. It is also important in connection with exoplanets since some of them (e.g. hot Jupiters) can be considered extreme cases of binary stars subject to extreme reflection effects. The reflection effect describes the mutual irradiation of the components in a binary system and, most importantly, the surface temperatures of the components and the radiation field. Because one of the components is typically relatively hot and temperatures on the irradiated side of the cool component can exceed 10 000 K, UV observations are key to our understanding of this effect.

There are models of the reflection effect with various degrees of sophistication and precision. Models that are used to calculate the light curves and spectra of eclipsing binaries are the most popular ([Wilson 1990](#)). They usually assume that the irradiated atmospheres radiate as non-irradiated ones, but with an enhanced effective temperature. Apart from that, some models take into account a parameterisation of heat redistribution over the surface

and scattered light (Budaj 2011b; Horvat et al. 2019). There are LTE and NLTE models of stationary irradiated atmospheres in radiative and convective equilibrium (Burrows et al. 2008; Vučković et al. 2016) revealing that irradiated atmospheres may have a very complicated structure with temperature inversions that can lead to the appearance of emission lines. Finally, there are hydrodynamic simulations of the process (Dobbs-Dixon & Lin 2008) indicating the presence of an equatorial jet carrying the heat from the irradiated to shadowed side.

Despite all these efforts on several fronts, there are plenty of open questions that need to be addressed, and UV observations of binaries with one hot (WD, sdB, sdO) and one cold component (a red dwarf or a red giant) will play a crucial role. For example: What is the amount of scattered light and albedo of the irradiated star? Why do some observed albedos of irradiated stars require values close to or larger than one? What is the efficiency of the heat transport from irradiated to nonirradiated side in (binary) stars/exoplanets? What is the structure and radiation field of the irradiated atmosphere? How does it affect the albedo, convection, shape of the star, gravity, and limb darkening (Ruciński 1969; Claret & Bloemen 2011)? How does the reflection effect affect stellar and planetary evolution? To answer these questions, multi-band observations with an SNR of about 100 with a time resolution of at least 5 minutes are needed.

3.7 Eclipsing binaries: a key to deriving bolometric corrections in the UV

Recently, eclipsing binaries with well-known physical parameters of the components were shown to be a very important tool to derive multi-band (Johnson B, V and Gaia G, G_{BP}, G_{RP}) bolometric corrections (Bakış & Eker 2022), which can be used to derive luminosities of the components with uncertainty as low as one percent. Eker & Bakış (2023) increased the number of photometric bands in their method from 5 to 6 by including the *TESS* (Ricker et al. 2014, 2015) bandpass to derive bolometric corrections for the *TESS* bandpass. They also showed that it is possible to derive luminosities and radii of single stars with an error of about 2 per cent, which is equivalent to values already published. Thus, increasing the number of bandpasses to achieve more reliable luminosity and radius of binary components and single stars is paramount. The key issue of this method is to obtain precise magnitudes in the desired bandpasses. It is obvious that using magnitudes of stars obtained in UV, which are only possible by systematic space-based observations of binary systems and/or single stars, will fill the gap on the UV side of the wavelength regime of the method described by Bakış & Eker (2022).

4 Mergers of intermediate masses

N-body simulations of Dvořáková et al. (2023) show that about 50% of the merger products of the binaries are B-type stars. The first post-merger in the phase when the envelope started to be transparent was found among FS CMa

stars (IRAS 17449+2320, [Korčáková et al. 2022](#)). FS CMa stars are a subgroup of stars showing the B[e] phenomenon, i.e., the presence of the forbidden emission lines and infrared excess ([Allen & Swings 1976](#); [Lamers et al. 1998](#)). These are indicators of a very extended circumstellar gas and dust region. Properties of several other FS CMa stars indicate that there may be more post-mergers hidden in this group. However, not every object in the list of FS CMa stars is a post-merger. The group was defined primarily on the basis of the infrared properties ([Sheikina et al. 2000](#); [Miroshnichenko et al. 2001](#); [Miroshnichenko 2007](#)), which is not a sufficiently sharp criterion. Therefore, the list contains several binaries (Be/X-ray binary CI Cam, [Barsukova et al. 2006](#); 3 Pup, [Miroshnichenko et al. 2020](#); GG Car, [Porter et al. 2021](#); AS 386, [Khokhlov et al. 2018](#); or MWC 349A, [Tafoya et al. 2004](#)), B[e] supergiant (MWC 300, [Appenzeller 1977](#)), and post-AGB candidates (Hen3-938, [Miroshnichenko et al. 1999](#), CPD-48 5215, [Gauba & Parthasarathy 2004](#)).

Figure 3 shows a model of a FS CMa post-merger. The central star is a magnetic B-/early A-type star. The magnetic field is generated by mixing during the merger ([Schneider et al. 2020](#)). It may reach high values (~ 6.2 kG in IRAS 17449+2320, [Korčáková et al. 2022](#)) that are comparable to the strongest fields in Ap stars. Such a strong magnetic field slows down the stellar rotation rapidly ([Schneider et al. 2020](#)) leading to the observed low rotation velocities (review in [Korčáková 2022](#)). The central star is probably a pulsator, where the resonance of individual pulsating modes may play a role. The star undergoes episodic material ejection approximately once a month. The geometrically extended gaseous disk is very inhomogeneous. Rotating arms and spots, as well as expanding layers, have been observed. The expanding layers slow down in some cases, even some material falls back onto the star ([Kučerová et al. 2013](#)). Behind this gaseous disk, one or two dust rings are present. Dust regions are very clumpy, even large dust clouds were detected around some stars ([de Winter & van den Ancker 1997](#)). The composition of these two rings may be different. Closer to the star, the graphite grains are present, whereas the outer region is composed of silicates ([Gauba et al. 2003](#); [Varga et al. 2019](#)). The object has an extended low-density “corona”, probably due to the very strong magnetic field ([Moranchel-Basurto et al. 2023](#)). Seeing this object from the equator, the strong absorption of iron-group elements appears in the UV spectrum, so-called “iron curtain”. The flux may be reduced by approximately an order of magnitude compared to the classical B-type star ([Korčáková et al. 2019](#)). The absorption lines of the lower excitation stages also appear in the spectrum, because the disk behaves as a “pseudo-atmosphere”. In this case, lines that should never be detected in B-type stars may be created. The most puzzling and important example is the Li I line resonance doublet ([Korčáková et al. 2020](#)). The UV excess instead of the UV depression may be observed from the polar regions ([Bergner et al. 1990](#); [Korčáková et al. 2022](#)).

The UV radiation is one of the key factors driving the variability in the visible and IR regions. The absorbed UV energy is redistributed to the longer wavelengths affecting not only the continuum, but also spectral lines. For

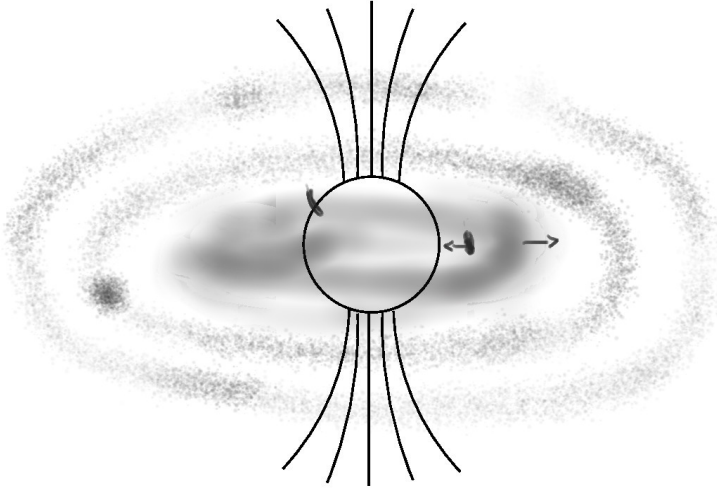


Fig. 3 Empirical model of a FS CMA post-merger. The slowly rotating strongly magnetic B-type star is surrounded by highly inhomogeneous gaseous region. Rotating spots, arms, and expanding regions have been observed, as well as the material infall and ejecta. Farther from the star, one or two dust rings are present. The dust region is very clumpy, even large clouds have been detected.

example, one of the related processes is connected with the overpopulation of upper levels. The follow-up cascade of radiative deexcitation leads to the appearance of the emission lines in the visible and IR. Without the knowledge of the behaviour of the UV radiation, it is hard to properly decode the information hidden in the spectral lines. Therefore, UV photometry is one of the essential techniques for the study such complex objects.

A precise description of the short-term variability on the scale from minutes to hours allows the search for pulsation modes of the central star. The interference of the pulsation modes, leading to the so-called beating phenomenon, may be responsible for ejecting matter in these stars. The determination of the pulsation modes is especially important in FS CMA post-mergers since these objects are still out of the thermal equilibrium as shown by simulations of Schneider et al. (2020) and position on the Hertzsprung–Russell diagram (Miroshnichenko 2017). On-time scales around seven hours, disk oscillations may be detected; similar to the disk flickering observed in cataclysmic variables (Bruch 2021) or symbiotic binaries (Sect. 3.3). To distinguish the disk oscillation from the stellar pulsations, two bandpasses are necessary since the flickering amplitude is wavelength-dependent.

The photometry on longer time scales in two bands allows one to follow the molecule and dust formation. Such an event has already been detected in MWC 349 (White & Becker 1985). Since the matter in the disk very efficiently absorbs the UV radiation, a raw guess of the angle of view is very easy to determine based on the detected UV excess/depression. The UV properties and its variability are one of the important ways to classify such a heterogeneous

group as FS CMA stars, which is the necessary requirement for the search of new post-mergers.

Even if only one intermediate-mass merger has been found yet in the phase when the envelope started to be transparent, these post-mergers definitely deserve more attention. As they represent the most frequent channel of mergers, their contribution to the enrichment of interstellar matter may be significant. They may also contribute to the enrichment of intergalactic matter since the simulations of [Dvořáková et al. \(2023\)](#) indicate that the merger may occur outside the home galaxy. The position of FS CMA stars in the Hertzsprung-Russell diagram ([Miroshnichenko 2017](#)), around the terminal-age-main-sequence, with the combination of the simulations of the merger event and evolution ([Schneider et al. 2020](#)) shows that FS CMA post-mergers are still out of thermal equilibrium. These objects offer an attractive opportunity to study and test stellar structure and evolution models. Last, but not least, less massive FS CMA post-mergers may be progenitors of magnetic Ap stars. Some of them may offer an explanation for appearance of strong magnetic field in young white dwarfs.

The requirements for the mission parameters depend on the scientific goal. While for the search for UV excess or deficiency one UV-band is sufficient, study of variability typically requires a combination of far-UV and near-UV bands. For most of the goals SNR of about 50–200 should be sufficient, but the study of short-term variability requires an SNR of up to 1000 and a cadence of 10 s.

5 Star Clusters and ISM

5.1 Photometric study of star clusters

Star clusters, especially young ones, are relatively unexplored in the UV. The understanding of the UV-bright stars and the populations they reside in – clusters and stellar associations – can be applied to study these objects in other galaxies. As we are only able to resolve the stellar populations in the relatively nearby galaxies (up to a few Mpc away), the understanding of the local clusters and associations dominated by UV-bright stars ([Siegel et al. 2019](#)) is crucial for studying these objects at extragalactic and cosmological distances, where they cannot be resolved. These distant populations are frequently metal-poor, so studying local (and those in the Magellanic Clouds) low-metallicity clusters and associations will be instrumental in testing of isochrones in the low-metallicity populations ([Chaboyer & Kim 1995](#)).

Many interesting types of stars (e.g. variables and binaries) can also be investigated in star clusters. In fact, it is preferable to investigate members of star clusters because we have additional knowledge about their reddening, distance, age, and metallicity. There are several types of unique objects that could be reliably identified only in star clusters, mainly due to their (unusual) position in the cluster colour-magnitude diagrams, where they pose as outliers that deviate from isochrones. Blue stragglers and extreme horizontal branch

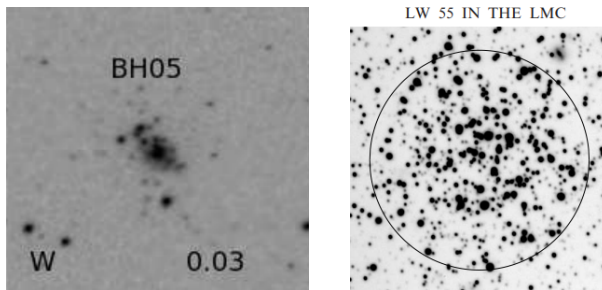


Fig. 4 Extra-galactic clusters in Andromeda Galaxy (left) and in the Large Magellanic Cloud (right). Images were taken from [Caldwell et al. \(2009\)](#) and [Kaluzny & Rucinski \(2003\)](#).

stars are good examples of such objects. Due to their scarcity, they are not well understood, and the evolutionary pathways that lead to their formation remain in doubt ([Michaud et al. 2011](#)). However, due to their high temperatures when compared to the turnoff point, they emit a copious amount of UV radiation, especially if the studied cluster is younger than about 1 Gyr. A UV mission that gathers photometry of these objects would provide helpful data that would supplement existing datasets and allow us to answer some open questions regarding these objects. For example, these include the formation scenarios for blue stragglers or extreme horizontal branch stars ([Jadhav & Subramaniam 2021](#)) and the role of binarity in the observed lack of white dwarfs in open clusters ([Bianchi et al. 2011](#); [Anguiano et al. 2022](#)).

When we look at a colour-magnitude diagram of a star cluster, we can usually identify the main-sequence turnoff (MSTO) point as the position of the bluest (lowest colour index) main-sequence star in the diagram. Since stars located above this point in the colour-magnitude diagram evolve away from the main sequence, astrophysicists use MSTOs to estimate the ages of star clusters. Because stellar rotation alters photometric indices and stars rotate with different velocities, star clusters show so-called extended main-sequence turnoff (eMSTO) ([Lim et al. 2019](#)). It has been suggested that some clusters have experienced prolonged star formation and that age variation, together with stellar rotation, is responsible for the eMSTOs ([Goudfrooij et al. 2017](#)). This effect has not been studied in UV so far. Since the effects of interstellar and differential reddening can be readily identified in UV ([Turner 1979](#); [de Meulenaer et al. 2014](#); [Legnardi et al. 2023](#)), investigating eMSTO in this part of the spectrum should help us to explain this effect.

The observations from *Swift* UVOT have shown that the isochrones constructed using UV bands do not match the photometry of the red giants and late-type main-sequence stars properly ([Smith & Cochrane 2020](#)). A possible explanation is that the atmospheric models are incomplete in their treatment of the UV absorption and emission lines originating due to circumstellar envelopes and chromospheric activity (Sect. 2.3). With the UV mission, the shortcomings of the current models could be tested.

The use of colour-magnitude diagrams in the determination of the cluster parameters is quite limited in the case of very distant Galactic and extragalactic clusters (for example, see Fig. 4), where resolving individual members is usually not possible (Piecka & Paunzen 2021). These problems can be overcome by using integrated photometry. Using nearby and resolved star clusters, one can calibrate integrated photometry in terms of age, reddening, and metallicity (Lata et al. 2002). With libraries based on population synthesis codes, it is also possible to determine the total mass and the fraction of red giants of star clusters (Bridžius et al. 2008). This method is well established, but it has not yet been applied to the UV region.

The photometric measurements of individual members of clusters in our Galaxy requires a reasonably narrow point spread function to distinguish between the individual stars. In general, we do not expect to reach distances larger than about 3 kpc, and anticipate more strict limitations within the extinction-dominated Galactic disk. Integrated photometry of star clusters can be conducted for local and extragalactic targets. For both objectives, the main bandpass should mostly cover the 200–300 nm region. A secondary band covering wavelengths unreachable from the ground (< 200 nm) would be beneficial. The FoV requirement is set by the size of the closest cluster included in such a study.

5.2 Deriving interstellar extinction in UV

Interstellar dust is an important component of the interstellar medium (ISM). Properties of the constituent particles are inferred from observations by studying extinction curves together with polarisation curves, scattered light, dust emission in the continuum, and absorption in bands (Draine 2003). Although an average extinction law is often assumed when deriving extinction-corrected magnitudes of stars, looking in different lines of sight shows variations in the shape of the extinction curve that are connected to changes in the properties of dust (Jenniskens & Greenberg 1993).

An extinction curve shows how the attenuation of light (measured, for example, by extinction A_λ) depends on wavelength (Fig. 5). This curve is affected not only by the chemical composition of the dust (mostly silicates, graphite, ices, and polycyclic aromatic hydrocarbons) but also by the sizes of the individual particles, ranging from a few microns down to a couple of nanometres (e.g., Weingartner & Draine 2001). The strongest feature of the extinction curve observed in near-UV is the extinction bump located at around 217.5 nm (Stecher 1965).

Based on IR photometric data, Larson & Whittet (2005) found that many high-latitude clouds in our Galaxy show signs of an increase in the number of smaller particles when compared with the diffuse ISM of the Galactic disk. Variation in the size distribution of dust grains should affect not only the strength of the UV extinction bump, but also the general steepness of the extinction curve in UV. This was explored by Sun et al. (2021), who made use of the UV data produced by the *GALEX* mission and found that such a

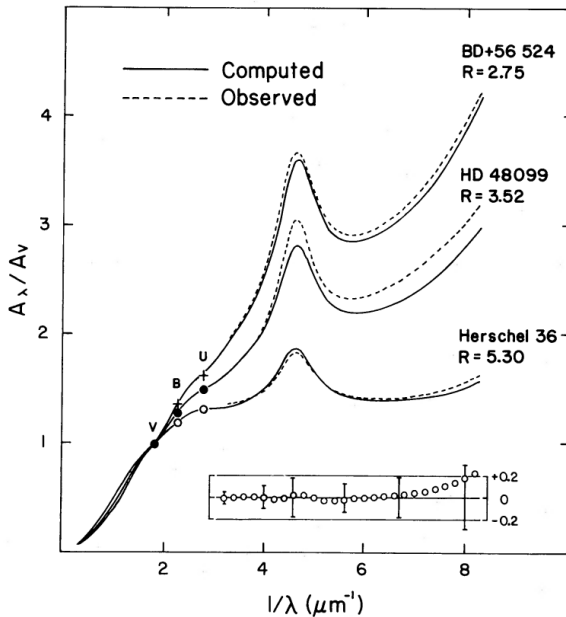


Fig. 5 Extinction curves for different lines of sight (Cardelli et al. 1989).

situation mostly occurs in clouds with a relatively small amount of extinction in the visible part of the spectrum.

A dedicated UV photometric survey would improve our understanding of this effect. Additionally, a good choice of photometric bands can help us to distinguish between the UV continuum extinction and the strength of the bump at 217.5 nm, allowing us to study the variations in the dust grain populations in better detail. This is important for different studies of the ISM that focus on variations in extinction curves, the evolution of dust grain populations, and the formation of molecules.

To maximize the scientific output, it would be ideal to fit as many targets in one field as possible – for this reason, it would be ideal to have a FoV larger than 1° . Magnitude errors should be smaller than 0.1 mag, ideally as small as 0.01 mag. While the survey can work with almost any bandpass in the 200–300 nm region, it would be preferred to make use of a band that is focused on the wavelengths between 220 nm and 280 nm, which should best help to capture the information about the profile of the UV extinction bump (when combined with the available magnitudes at longer wavelengths). A second band centred at slightly longer (~ 340 nm) or shorter (~ 160 nm) wavelengths would be beneficial to this study. The far-UV band is preferred because it provides more information.



Fig. 6 Composite UV images of bow shocks in the vicinity of Mira (left) and CW Leo (right) taken by *GALEX*. Downloaded from <https://galex.stsci.edu/GR6/>.

5.3 Getting information about the ISM from UV bow shocks

There are multiple events that can lead to the formation of shock waves in the ISM. One of them is the movement of a star with a strong stellar wind and a high velocity with respect to the local ISM (e.g. [van Buren & McCray 1988](#)). The resulting bow-shaped shocks (or bow shocks) can be observed at various wavelengths, most notably in the infrared ([Li & Draine 2001](#); [Draine & Li 2007](#)), optical ([Brown & Bomans 2005](#)), and at the higher energies as well. In a few cases UV-emitting bow shocks have been found, for example, around Betelgeuse ([Decin et al. 2012](#)), Mira ([Martin et al. 2007](#)), and CW Leo ([Ladjal et al. 2010](#)) (see Fig. 6).

However, the UV emission of bow shocks is not well-constrained since their observation in this spectral region is quite challenging. Firstly, their driving stars are often strong UV emitters, making it difficult to resolve the rather faint, diffuse, and wispy emission of a bow shock in their proximity. Moreover, some missions such as *GALEX* intentionally avoided many bright UV stars, in order to protect its detectors ([Choi et al. 2015](#)). Some bow shocks from [Gvaramadze et al. \(2010, 2011\)](#); [Kobulnicky et al. \(2016\)](#) were serendipitously observed by *Swift* UVOT, but so far no clear bow shock emission associated with O and B stars has been detected in UV.

Detecting these structures in UV would provide valuable data to complement the observations more routinely done in other bandpasses. One of the main focuses would be to put constraints on the physical processes that dominate in the bow shock regions. Several processes may influence the bow shock emission in UV, including absorption ([Decin et al. 2012](#)) and scattering by dust particles, emission lines resulting from collisional excitation ([Martin et al. 2007](#)), and to a smaller degree also, inverse Compton scattering ([del Valle & Pohl 2018](#)).

The bow shocks can be detected from frame images focused on regions surrounding asymptotic giant branch (AGB) stars, and O and B stars. Since the angular radius of a bow shock depends on the distance (and other parameters), a reasonable FoV ($\sim 1^\circ$) is required. The angular resolution should be sufficiently high to be able to map the structure of the bow shocks. The magnitude limit is mostly influenced by the observability of O and B stars. While most of the AGB stars are expected to have $m_{UV} > 9$ mag, O-type stars of interest have $m_{UV} > 4$ mag (if we focus on objects beyond 1 kpc, $m_{UV} > 6$ mag). For this reason, it could be possible to allow having the observed objects saturated in some cases. To be able to identify bow shocks, the signal-to-noise ratio has to be higher than 3. Although an AGB star at 3 kpc could be as bright as $m_{UV} = 16$ mag, the situation changes when the presence of the ISM is assumed, which would shift the lower limit to $m_{UV} \geq 20$ mag.

GALEX images suggest that UV bow shocks appear brighter at shorter wavelengths. While some results are already expected for a near-UV region, a far-UV band should enable the identification of more bow shocks.

6 Exoplanets

In the past three decades, the characterization of thousands of extra-solar planets allowed us to make further steps towards the understanding of the origin of life on Earth and the possible discovery of signs of life outside our Solar System. In terms of methodology, numerous techniques have proven to be useful for confirming the presence of a planet orbiting a distant star, such as pulsar timing variations (Wolszczan & Frail 1992), radial velocity measurements (Mayor & Queloz 1995) or direct imaging (see, e.g. Lagrange et al. 2020). However, the vast majority of known systems were discovered and investigated via photometric measurements of planetary transits, i.e. when the planet blocks a small but well-detectable amount of stellar light in coincidence with its orbital period (Henry et al. 2000). The dominance of transiting planets within the family of known planets is mostly due to the significant advantage of spaceborne photometry: it yields not just precise and accurate time series, but the lack of diurnal variations allows for the extension of the time domain compared to ground-based telescopes. Therefore, space telescopes play an important role in the analysis of these systems.

6.1 Transiting exoplanetary systems

While radial velocity measurements are essential to derive the mass ratios and orbital characteristics of exoplanetary systems, the information provided by photometric transits (and occultations) significantly increases our knowledge by revealing the size and, therefore, the density of the planets. The first such confirmation of the presence of transits happened in the case of the planetary system HD 209458(b) (Charbonneau et al. 2000) while, a few years later, the transit method was applied for the discovery of OGLE-TR-56 (Konacki et al. 2003). In addition, precise time series associated with individual transits not

only reveal a more precise orbital solution in terms of parameters such as orbital period or inclination, but also play a key role in understanding the host star (Seager & Mallén-Ornelas 2003). Although these key discoveries and confirmation of transits were also made by space-borne photometry (see, e.g. Brown et al. 2001), dedicated space missions such as *CoRoT* (Barge et al. 2008), *Kepler* (Borucki et al. 2010) or *TESS* (Ricker et al. 2015), literally increased the number of known such systems by thousands.

Similarly to our Solar System, perturbations occur between different planets orbiting the same star. By their nature, such perturbations are highly dependent on the mass of the planets. One of the most easily and precisely observable effect of such perturbations is the variation in the orbital phase of the planetary companions. Periodic or systematic variations in the orbital phases cause measurable changes in the transit timings. Observations of these transit timing variations allow us to determine the masses of the planets (Holman et al. 2010). In addition, perturbations having an intrinsically secular nature also yield observable changes in the duration of the transit. For instance, the oblateness of the host star causes the planetary orbit to precess, implying a slight but detectable systematic shift in the duration of the transits (Szabó et al. 2012). Such measurements therefore reveal intrinsic parameters of the host star, like the non-spherical components of its gravitational field. Taking into account the variations in the parameters of exoplanetary systems, such as transit timing variations or transit duration variations, it is also possible to reveal the presence of another companions that would otherwise remain undetected. This is particularly relevant for companions on orbits with lower inclinations, on which the exoplanets do not transit the star, or have so small masses that they do not provide sufficiently high amplitude signals in radial velocities.

The shape of transit light curves are also determined by the stellar limb darkening (see, e.g. Brown et al. 2001). Quantitatively, the limb darkening depends on both the central wavelength of the observations and the stellar atmospheric parameters (Claret 2004), allowing further refine the host star parameters (such as the independent measurements of the surface temperature or spectral type). Limb darkening is more prominent on shorter wavelengths. Precise space-borne observations are important to manage the correlations between the planetary radius and the derived limb darkening parameters (Pál 2008). In addition, the presence of an atmosphere can yield a wavelength-dependent planetary radius (see, e.g. Deming et al. 2019, for an introduction). Stellar spots also affect transiting light curves (Nutzman et al. 2011; Oshagh et al. 2013), and the shorter the wavelength used for observation, the greater the contrast the stellar spots have, allowing a clear distinction of stellar spots from instrument noise.

The study of exoplanetary transits is relatively demanding for the mission parameters. The requested SNR of about 500 within one-hour exposition could be accordingly modified if faster cadence of about 1 min is needed.

6.2 Activity, flares, and star-planet interaction

By nature, flares, and the corresponding physical processes (such as coronal mass ejections) associated with a star harbouring a planetary system affect habitability: the higher the flaring rate, the more energetic the ionizing radiation threatening the potential life on a planet. On the other hand, having no flaring activity on a host star might not provide sufficient input for triggering the formation of fundamental molecules essential to life. Main-sequence stars with a small mass (i.e. mostly M dwarfs or K dwarfs) are the focus of research in the field of exoplanets due to the easier detection of planetary companions (see, e.g. [Irwin et al. 2011](#), and the references therein). These objects tend to have an enormous amount of flaring activity, as shown by recent individual ([Vida et al. 2019](#)) and statistical ([Seli et al. 2021](#)) analyses. While observatories like *TESS*, operating at long wavelengths, provide reliable constraints in a statistical manner for a large number of objects (see also [Seli et al. 2021](#)), flaring activity is the most prominent at short wavelengths, such as the UV band (Sect. 2.3).

It is well known that stars strongly affect their close cool companions via gravity and irradiation (see, e.g. Sect. 3). It is less obvious that planets also affect their host stars. Late-type stars store a significant amount of energy in their surface magnetic fields. Giant planets on close orbits may have their own magnetic fields and magnetospheres that may interact with the stellar magnetic fields (see [Vidotto 2020](#), for a review). As the planet moves over the surface of the star, it may trigger reconnection events that will follow the planet. This may heat the upper atmosphere of the star and cause variability with a period equal to the orbital period of the planet. Apart from that, the stellar wind may interact with the planetary magnetic fields, creating a bow shock and an asymmetry in the circumplanetary material. This was detected as an early ingress during the transit of WASP-12b in UV with the Hubble Space Telescope (*HST*) ([Fossati et al. 2010](#)). Detection of this kind of interaction is important because it would provide information on the magnetic field of the planet, which is almost impossible to obtain by other methods. The magnetic field of the planet is crucial for the assessment of the habitability of the planet.

UV photometry is particularly well suited to study such planet-star interactions. This is because UV flux originates from the upper atmosphere. UV flux of late-type stars constitutes only a small fraction of their total energy output. Hence, the UV band is very sensitive to such high-energy phenomena even if the flux in the visual band remains almost constant. Study of planet-star interactions will require monitoring of about a dozen stars with massive close-in planets for weeks. This task is too expensive for large telescopes such as *HST* and small-scale missions such as *QUVIK* can make a significant contribution in this field.

6.3 Exo-atmospheres at short wavelengths – the border between life and death

UV photometric mission will offer a unique window into the characterization of exoplanetary atmospheres. The energetic radiation heats the upper layers of planetary atmospheres, making the atmospheric material easier to escape. In the UV part of the electromagnetic spectrum, the planetary diameter appears larger, and thus transits are deeper than at longer wavelengths. This allows us to study the evaporation of atmospheres and atmospheric escape, which is particularly strong in close-in planets around M-dwarf stars (for example, GJ436 b, [Ehrenreich et al. 2015](#); [Lavie et al. 2017](#)).

There is a well-known gap in the radius distribution of exoplanets ($1.6 - 2 R_{\text{Earth}}$) and a complete lack of Neptun-sized exoplanets with orbital periods shorter than 3 days (e.g. [Howard et al. 2012](#); [Sanchis-Ojeda et al. 2014](#); [Fulton et al. 2017](#); [Van Eylen et al. 2018](#)). This is explained as a result of exoatmospheric erosion and has been predicted by many different escape models (e.g. [Lopez et al. 2012](#); [Ginzburg et al. 2018](#)). Observations by small-sized UV telescopes will help us to understand the atmospheric escape better and give us a better idea of the capability of the planets to keep their atmospheres. This is especially important in studying exoplanets in habitable zones that could potentially host extraterrestrial life.

7 Transiting dusty objects: from exoasteroids to dusty discs

Dust is known to scatter and absorb UV radiation very efficiently. At the same time, hot stars are strong emitters of UV radiation. Consequently, UV telescopes are ideal for detecting and studying transits of dust clouds in front of sufficiently bright and hot stars. While the nature and origin of stars and dust are usually specific to a given type of star, the dust obscuration process is universal.

7.1 Disintegrating exoplanets

Most of the known exoplanets transit their host stars and feature stable and symmetric transits. A decade ago, a new class of objects was discovered ([Rappaport et al. 2012](#)) that exhibit asymmetric, strongly variable but periodic transit-like signals. Sometimes they feature a strange pre-transit brightening. Kepler-1520b became a prototype of such objects. On the other hand, some transits, such as those of K2-22b ([Sanchis-Ojeda et al. 2015](#)), look almost the opposite, with a post-transit brightening. Periods are shorter than one day, and transit durations are approximately 1 hour.

It turned out that such transits are caused by disintegrating exoplanets that orbit very close to their host stars. The rocky surface of the planet evaporates and forms an opaque dusty tail. It is this tail that is causing the transit, while the planet itself is usually too small to be detected. The tail (dust cloud)

is very sensitive to various processes, such as radiative/gravitational accelerations, dust evaporation, or condensation. It efficiently scatters the radiation in the forward direction, causing the above-mentioned pre- or post-transit brightenings, depending on whether the tail is trailing or leading the planet. Such planets might have lost a significant fraction of their mass, exposing their naked cores (Perez-Becker & Chiang 2013). Consequently, the properties of the dust tail reflect the bulk (not only the surface) chemical composition of the planet and provide a unique tool for probing the interiors of the planet.

There are half a dozen of such objects. Generally, their transits would be difficult to detect in UV since stars are typically of later spectral types (F-M), faint ($V = 16$ mag), and the transit depth is often below 1%. However, there are related objects that are either brighter and/or the transits are deeper, and these are mentioned in Sect. 7.2.1. Ongoing and planned space missions such as *TESS* (Ricker et al. 2015) and *PLATO* (Rauer et al. 2014) may discover brighter objects of this kind.

7.2 Exoasteroids

Since the discovery of disintegrating exoplanets, even smaller (minor) bodies have been detected to orbit and transit other stars – “exoasteroids”. White dwarfs offer an advantage in detecting such objects. Their radii are 100 times smaller than the Sun, which enables the detection of relatively small objects. The first known exoasteroids were discovered orbiting a white dwarf named WD1145+017 (Vanderburg et al. 2015, WD1145). They have orbital periods of about 4–5 hours, and transits in the optical region may be 40–60% deep. An example of the light curve from the 2017 season is shown in Fig. 7. One can see numerous dust clouds associated with asteroids passing in front of the star, causing eclipses. This behaviour is in many respects similar to the disintegrating exoplanets mentioned above. The nature and variability of such transits call for simultaneous multi-wavelength observations to put constraints on the chemical composition and properties of dust. Surprisingly, UV observations unravelled that transits at these wavelengths are significantly shallower than those in the optical region (Hallakoun et al. 2017; Xu et al. 2019). The reason for that is still an open question, but it may be a combination of two factors: an underlying absorption by a co-planar gas disk and a forward scattering on large dust particles (Xu et al. 2019; Budaj et al. 2022).

The discovery of such exoasteroids solves a missing chain in our understanding of the chemical composition of white dwarfs. Many white dwarfs show heavy elements in their spectra. However, these elements should have quickly sunk due to the strong gravity of the star (Paquette et al. 1986). WD1145 unravelled the expected chain of events before our eyes for the first time (Debes & Sigurdsson 2002): stars have planetary systems; orbits of bodies are disturbed by mass loss during the AGB phase; they get close to the WD (a remnant of the AGB star) and are disrupted into pieces, forming dust clouds; dust turns into a gaseous disk as it approaches the hot star; and, finally,

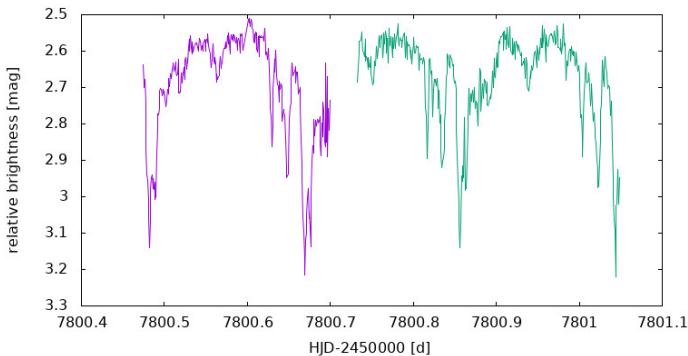


Fig. 7 Light curve of WD1145 in the optical region observed in 2017 (Maliuk et al., in preparation). Everything deeper than an uncertainty (0.02 mag) are transits.

gas accretes onto the surface of the star, contaminating its chemical composition. Consequently, by measuring the chemical composition of the star or its gaseous disk, we also infer the chemical composition of the disrupted body. For example, it appears that WD1145 recently encountered and accreted a body of Earth-like composition (Xu et al. 2016; Fortin-Archambault et al. 2020; Budaj et al. 2022).

The characteristic time scale and the amplitude of variability due to transits of exoasteroids are 10 minutes and 0.1 mag, respectively. Required SNR and cadence are 50 and 2 min, respectively. An advantage of such white dwarfs is that they are hot (characteristic spectral type is DB) but relatively faint ($U = 17\text{--}18$ mag).

Since the discovery of WD1145, there has been increasing evidence that asteroids, planets or their remnants are also orbiting other white dwarfs: ZTF J013906.17+524536.89 (Vanderbosch et al. 2020), SDSS J122859.93+104032.9 (Manser et al. 2019), and WD J091405.30+191412.25 (Gänsicke et al. 2019). Most recently, a Jupiter size planet was directly detected to transit WD 1856+534 (Vanderburg et al. 2020). However, there are still only a handful of such objects, and little is known about their incidence, orbits, masses, chemical composition, evolution, origin, and other properties. Increasing these numbers is a crucial next step in answering all these questions. A small UV telescope may be used to search for such variability by targeted observations of selected white dwarfs, by post-processing of full-frame images, or for follow-up observations of new objects detected by other missions (*TESS*, *PLATO*).

UV photometry will verify the nature of the event. Dust clouds will have variable asymmetric transits of different depths at different wavelengths. Based on the shape of the transit, it will be possible to put constraints on the shape of the dust cloud (e.g. trailing/leading tail, disk).

Dust properties, such as particle sizes and chemical composition, are another important question that requires multi-wavelength observations. UV photometry in two bandpasses will constrain these properties. However, since

the depths of transits are variable, they will have to be coordinated with additional simultaneous observations in the optical and IR regions. Apart from that, it will be possible to put constraints on the total amount of dust and its production rate, which will constraint the masses and lifetimes of the dust-producing bodies.

An advantage of the UV region is that it is most sensitive to small dust particles ($< 0.1 \mu\text{m}$) that are difficult to detect at longer wavelengths. Consequently, transits may be deeper in the UV region and may not even be seen at other wavelengths.

7.2.1 Related objects

There are stars that are brighter than the above-mentioned white dwarfs and are related to the topic. Boyajian's star (Boyajian et al. 2016) is a famous example. It is an F-type and $V = 12$ mag star. Its Kepler light curve shows a few strong dimming events that are 10–20% deep, asymmetric, and aperiodic. Ground-based follow-up observations revealed multiple dips of about 1% (Boyajian et al. 2018). It is a 'normal' star on the main sequence, not a young star. Multi-wavelength observations indicate that this variability is compatible with a dust extinction caused by a swarm of comets (Bodman & Quillen 2016) or dust clouds associated with more massive bodies such as asteroids (Neslušan & Budaj 2017). *TESS* and *PLATO* missions should discover more objects of this kind. Characteristic timescale and amplitude of variability are 1 day and 0.01–0.1 mag, respectively. This translates into SNR of about 200 and the cadence < 1 day that is required.

7.3 Eclipses by dusty disks and rings

There are also other dusty objects much larger than the aforementioned minor bodies that transit stars. Some long-period eclipsing binary stars have very peculiar, variable, and asymmetric eclipses such as ϵ Aur (spectral type F0, $V = 2.9$ mag). It is a bright binary star with an orbital period of 27 yr and deep eclipses lasting for almost 2 yr (Ludendorff 1903). The fascinating story of this star dates back 200 years and is full of challenges, twists, and turns. The binary consists of a giant F star and a mysterious huge invisible component. Only multi-wavelength and interferometric observations during the latest eclipse proved the nature of the companion, which is a cool dusty disk (Kloppenborg et al. 2010). Nevertheless, it was widely believed that the disk was inclined to the orbital plane and that the light from the F star penetrated through the central hole in the disk, causing mid-eclipse brightening (Wilson 1971; Carroll et al. 1991). Surprisingly, it was shown that a co-planar but flared disk geometry (with a vertical thickness increasing with distance) and forward scattering could explain the strange eclipse more naturally (Chadima et al. 2011; Budaj 2011a). Such objects are rare, and we know of only a few long-period binaries with such dusty disks. However, their numbers are growing, and most of them were discovered only during the last decade, thanks to modern

surveys and their combination with digitised archival data dating back more than a century. The nature/origin of their variability, central stars, disks, and properties (shape, dynamics, dust particle sizes, and chemical composition) are still a matter of debate. The characteristic duration and amplitude of variability are 1 yr and 0.1–1 mag., respectively. The SNR and the cadence required are about 100 and 1–10 days, respectively.

From the shape, duration, and variability of the eclipse, it will be possible to identify disks, rings, holes, gaps, clouds, or warps if present. Some of these structures may be associated with otherwise invisible small bodies orbiting inside the disk, which is interesting from the point of view of the planet formation (Kenworthy & Mamajek 2015). An advantage of the UV region is, again, that it is more sensitive to dust, and it may detect smaller dust particles that are invisible at longer wavelengths. If the UV observations are combined with observations at other wavelengths¹, this will put constraints on the dust particle size, its chemical composition, and the total mass of the dust.

Apart from that, observations in the UV region may help solve the main problem: what is inside the dusty disk? The light from this embedded object is heavily attenuated by the disk, which makes it difficult to detect the object. However, if this is a hot object, the disk atmosphere will efficiently scatter its UV light towards the observer, and the object may be detected in UV. During the eclipse, the main source of the light is suppressed, which further facilitates the detection of the hidden, hot object. This can be used not only for dusty but also for gaseous disks. UV photometry can be combined with spectroscopy, interferometry, and photometry at other wavelengths, to get a deeper insight into the structure of the whole system (Brož et al. 2021).

Another similar class of objects on a completely different scale are possible transiting circum-planetary (exoplanetary) rings or exorings. The presence of such rings has been recently hypothesised for some transiting exoplanets. It is related to the problem that the radii of some exoplanets are so large that their average densities are of the order of 0.1 g/cm³, which is an unexpectedly low value. The presence of exorings around these planets is an alternative solution of this problem (Akinsanmi et al. 2020; Piro & Vissapragada 2020). UV and IR observations are of crucial importance for detecting such rings. From optical observations alone, it is almost impossible to distinguish whether the transit is due to a seemingly large planet or a small planet with a dusty ring. An example is the exoplanet HIP 41378 orbiting a bright ($V=8.9$ mag) F8-type star (Akinsanmi et al. 2020).

There are also other fascinating events/stars in this category. One of the biggest and brightest stars in the sky, a red supergiant star Betelgeuse (spectral type M1 Ia, $V = 0.0$ mag), recently dimmed unexpectedly by a factor of 3, reaching a historical minimum in 2020 (Guinan et al. 2020). An increased UV continuum was observed prior to the dimming. The nature/origin of the variability is an open question. There were speculations about an imminent supernova eruption. However, UV observations with HST indicated that it

¹For example ZTF data covering optical region (Bellm et al. 2019) may be very useful.

could be due to a dust cloud passing in front of the star (Dupree et al. 2020). Another question arises about the origin and properties of the dust cloud. It might have originated from the star itself (see also Sect. 2.7). UV observations would be valuable, since the IR observations did not detect any significant change in brightness (Gehrz et al. 2020; Jadrlovský et al. 2023). Characteristic duration and amplitude of variability are 1 month and 1 mag. This translates into SNR and cadence that are required of about 100 and 1 week, respectively.

R Coronae Borealis (RCB) stars are another type of supergiants featuring irregular, several magnitudes deep fading events that may last for months or years. They are of spectral type F-G, hydrogen-poor, carbon-rich, and eclipses are most likely caused by the dust condensation in the vicinity of the star, but the nature of the stars and the events are not clear.

7.4 Dippers

Young dipper stars experience eclipses by dusty disks too. About 20–30% of classical T Tau stars are dippers (Alencar et al. 2010; Morales-Calderón et al. 2011). Most of these young stars are of late spectral types (K–M) and feature dusty protoplanetary disks. Such a disk may have a complicated structure with an inner disk that is misaligned with the outer disk. Day-long eclipses are often observed in these stars. It is believed that they are caused by dust from the inner disk that is nearly edge-on, causing an occultation of the star. Consequently, the light curve is very sensitive to any dust clumps at the edges of the inner disk. However, the nature of these dust clumps is unknown. They may be due to warps in the inner disk, vortices, or clumps associated with planet formation (Ansdell et al. 2016) or may be associated with magnetospheric accretion (Bodman et al. 2017). Dips may be quasi-periodic or aperiodic. The characteristic duration and the amplitude of the variability are 1 day and 0.1 mag, respectively. The required SNR is about 100 and a cadence of about a few hours.

There is another group of young stars called UXors after the prototype UX Ori. They are very similar to the above-mentioned dipper stars but are slightly more massive, hotter, and are often associated with Herbig Ae/Be stars (Grinin et al. 1991). They feature an infrared excess indicating a dusty disk, semi-regular dimmings on the time scales of months to years, and possible brightenings due to accretion or rotational modulation of variability due to spots.

Long-term multi-wavelength photometry will determine a possible periodicity of the events and put constraints on the geometry of the inner disk and dust clouds. In the case that the dips are periodic, it will be possible to locate their source based on the period. This may lead to the discovery of dust clouds or holes associated with planet formation. UV observations will be quite sensitive to such structures. They are also ideal for detecting hot spots on the surface of the star and determination of the rotational period of the star. Such spots are associated with magnetospheric accretion, which, in turn, indicates the presence of magnetic fields. This will put important constraints on

the corotation and Alfvén radii that control the magnetospheric accretion and eventually shed more light on the origin of dips.

Typical dipper stars (Ansdell et al. 2016) are K–M stars with J magnitudes in the range 8–13 mag, which corresponds to U magnitudes of about 14–19 mag. Consequently, those dipper stars and UXors that are brighter and hotter should be observable with a small UV telescope.

Multi-wavelength observations will also put constraints on the dust properties and chemical composition. Using two bandpasses in UV would help to constrain the temperature of the star from the slope of its continuum. However, since most of these dipper stars are of late spectral types and faint, we do not expect to detect many of them in the far-UV band.

8 Conclusions

We have demonstrated the impact of a small-size two-band UV photometric satellite on the astrophysics of stars and stellar systems. We have shown that UV mission can improve our understanding of physics and evolution of virtually all types of stars, including hot and cool main-sequence stars, supergiants, and compact remnants such as neutron stars. UV photometry provides constraints for precise determination of binary parameters, probes the circumbinary environment, and leads to significantly better understanding of different evolutionary stages of binaries including stellar mergers. Most conveniently, stellar physics can be tested for members of star clusters taking advantage of the common distance of all its members. UV mission can provide crucial information on exoplanets, including their basic parameters, atmospheres, and especially their interaction with host stars. UV observations can probe also other parts of exoplanetary systems from exoasteroids to large dusty disks.

Ground-braking observations can be obtained already using a single-band UV mission. However, we have demonstrated that including a second band can tremendously increase the scientific output of the mission. The optimal combination includes far-UV and near-UV bands.

We have listed the requirements that the satellite should met to fulfill individual scientific goals. The required parameters include the limiting magnitudes, final signal to noise ratio, and cadence of observations.

Acknowledgement

JBu was supported by VEGA 2/0031/22 and APVV-20-148 grants. JBe acknowledges support from the German Science Foundation (DFG) projects BU 777-17-1 and BE 7886/2-1.

Declarations

Competing Interests

The authors declare no competing interests.

References

- Abramkin, V., Pavlov, G. G., Shibanov, Y., & Kargaltsev, O. 2022, *ApJ*, 924, 128
- Aerts, C., Símón-Díaz, S., Bloemen, S., et al. 2017, *A&A*, 602, A32
- Akinsanmi, B., Santos, N. C., Faria, J. P., et al. 2020, *A&A*, 635, L8
- Akras, S., Guzman-Ramirez, L., Leal-Ferreira, M. L., & Ramos-Larios, G. 2019, *ApJS*, 240, 21
- Alencar, S. H. P., Teixeira, P. S., Guimarães, M. M., et al. 2010, *A&A*, 519, A88
- Allen, D. A. & Swings, J. P. 1976, *A&A*, 47, 293
- Allred, J. C., Hawley, S. L., Abbett, W. P., & Carlsson, M. 2006, *ApJ*, 644, 484
- Andersen, J. 1991, *A&A Rev.*, 3, 91
- Anguiano, B., Majewski, S. R., Stassun, K. G., et al. 2022, *AJ*, 164, 126
- Ansdell, M., Gaidos, E., Rappaport, S. A., et al. 2016, *ApJ*, 816, 69
- Antoniadis, J., Freire, P. C. C., Wex, N., et al. 2013, *Science*, 340, 448
- Appenzeller, I. 1977, *A&A*, 61, 21
- Auvergne, M., Bodin, P., Boissard, L., et al. 2009, *A&A*, 506, 411
- Ayres, T. R., Marstad, N. C., & Linsky, J. L. 1981, *ApJ*, 247, 545
- Baade, D., Rivinius, T., Pigulski, A., et al. 2016, *A&A*, 588, A56
- Bakiş, V. & Eker, Z. 2022, *Acta Astron.*, 72, 195
- Baliunas, S. L., Donahue, R. A., Soon, W. H., et al. 1995, *ApJ*, 438, 269
- Balona, L. A. 2011, *MNRAS*, 415, 1691
- Balona, L. A. 2017, *MNRAS*, 467, 1830
- Barge, P., Baglin, A., Auvergne, M., et al. 2008, *A&A*, 482, L17
- Barnard, M., Venter, C., Harding, A. K., Kalapotharakos, C., & Johnson, T. J. 2022, *ApJ*, 925, 184
- Barsukova, E. A., Borisov, N. V., Burenkov, A. N., et al. 2006, *Astronomy Reports*, 50, 664
- Basu, S. 2018, in *Astronomical Society of the Pacific Conference Series*, Vol. 515, *Workshop on Astrophysical Opacities*, 13
- Bedding, T. R., Mosser, B., Huber, D., et al. 2011, *Nature*, 471, 608
- Belczyński, K., Mikołajewska, J., Munari, U., Ivison, R. J., & Friedjung, M. 2000, *A&AS*, 146, 407
- Belkacem, K., Goupil, M. J., Dupret, M. A., et al. 2011, *A&A*, 530, A142
- Bellm, E. C., Kulkarni, S. R., Graham, M. J., et al. 2019, *PASP*, 131, 018002
- Bergner, Y. K., Miroshnichenko, A. S., Sudnik, I. S., et al. 1990, *Astrofizika*, 32, 203
- Bianchi, L., Herald, J., Efremova, B., et al. 2011, *Ap&SS*, 335, 161
- Blomme, R., Mahy, L., Catala, C., et al. 2011, *A&A*, 533, A4
- Bodman, E. H. L. & Quillen, A. 2016, *ApJ*, 819, L34
- Bodman, E. H. L., Quillen, A. C., Ansdell, M., et al. 2017, *MNRAS*, 470, 202
- Borucki, W. J., Koch, D., Basri, G., et al. 2010, *Science*, 327, 977
- Boyajian, T. S., Alonso, R., Ammerman, A., et al. 2018, *ApJ*, 853, L8
- Boyajian, T. S., LaCourse, D. M., Rappaport, S. A., et al. 2016, *MNRAS*, 457, 3988
- Bridžius, A., Narbutis, D., Stonkutė, R., Deveikis, V., & Vanevičius, V. 2008, *Baltic Astronomy*, 17, 337
- Brogaard, K., VandenBerg, D. A., Bruntt, H., et al. 2012, *A&A*, 543, A106
- Brož, M., Mourard, D., Budaj, J., et al. 2021, *A&A*, 645, A51
- Brown, D. & Bomans, D. J. 2005, *A&A*, 439, 183
- Brown, T. M., Charbonneau, D., Gilliland, R. L., Noyes, R. W., & Burrows, A. 2001, *ApJ*, 552, 699
- Bruch, A. 2021, *MNRAS*, 503, 953

- Budaj, J. 2011a, *A&A*, 532, L12
- Budaj, J. 2011b, *AJ*, 141, 59
- Budaj, J., Maliuk, A., & Hubeny, I. 2022, *A&A*, 660, A72
- Burrows, A., Budaj, J., & Hubeny, I. 2008, *ApJ*, 678, 1436
- Caldwell, N., Harding, P., Morrison, H., et al. 2009, *AJ*, 137, 94
- Cardelli, J. A., Clayton, G. C., & Mathis, J. S. 1989, *ApJ*, 345, 245
- Carroll, S. M., Guinan, E. F., McCook, G. P., & Donahue, R. A. 1991, *ApJ*, 367, 278
- Chaboyer, B. & Kim, Y.-C. 1995, *ApJ*, 454, 767
- Chadima, P., Harmanec, P., Bennett, P. D., et al. 2011, *A&A*, 530, A146
- Charbonneau, D., Brown, T. M., Latham, D. W., & Mayor, M. 2000, *ApJ*, 529, L45
- Chatterjee, P., Nandy, D., & Choudhuri, A. R. 2004, *A&A*, 427, 1019
- CHIME/FRB Collaboration. 2020, *Nature*, 587, 54
- Choi, Y.-J., Min, K.-W., & Seon, K.-I. 2015, *ApJ*, 800, 132
- Christophe, S., Ballot, J., Ouazzani, R. M., Antoci, V., & Salmon, S. J. A. J. 2018, *A&A*, 618, A47
- Claret, A. 2004, *A&A*, 428, 1001
- Claret, A. & Bloemen, S. 2011, *A&A*, 529, A75
- Claret, A. & Torres, G. 2018, *ApJ*, 859, 100
- de Meulenaer, P., Narbutis, D., Mineikis, T., & Vansevičius, V. 2014, *A&A*, 569, A4
- De Ridder, J., Barban, C., Baudin, F., et al. 2009, *Nature*, 459, 398
- de Winter, D. & van den Ancker, M. E. 1997, *A&AS*, 121, 275
- Debes, J. H. & Sigurdsson, S. 2002, *ApJ*, 572, 556
- Decin, L., Cox, N. L. J., Royer, P., et al. 2012, *A&A*, 548, A113
- del Valle, M. V. & Pohl, M. 2018, *ApJ*, 864, 19
- Deming, D., Louie, D., & Sheets, H. 2019, *PASP*, 131, 013001
- Dharmawardena, T. E., Mairs, S., Scicluna, P., et al. 2020, *ApJ*, 897, L9
- Dobbs-Dixon, I. & Lin, D. N. C. 2008, *ApJ*, 673, 513
- Doyle, J. G., Byrne, P. B., & van den Oord, G. H. J. 1989, *A&A*, 224, 153
- Draine, B. T. 2003, *ARA&A*, 41, 241
- Draine, B. T. & Li, A. 2007, *ApJ*, 657, 810
- Dupree, A. K., Strassmeier, K. G., Matthews, L. D., et al. 2020, *ApJ*, 899, 68
- Dvořáková, N., Dinnbier, F., Korčáková, D., & Kroupa, P. 2023, in preparation
- Ehrenreich, D., Bourrier, V., Wheatley, P. J., et al. 2015, *Nature*, 522, 459
- Eker, Z. & Bakış, V. 2023, *MNRAS*, 523, 2440
- Fekel, F. C., Moffett, T. J., & Henry, G. W. 1986, *ApJS*, 60, 551
- Fortin-Archambault, M., Dufour, P., & Xu, S. 2020, *ApJ*, 888, 47
- Fossati, L., Haswell, C. A., Froning, C. S., et al. 2010, *ApJ*, 714, L222
- Froning, C. S., Kowalski, A., France, K., et al. 2019, *ApJ*, 871, L26
- Fulton, B. J., Petigura, E. A., Howard, A. W., et al. 2017, *AJ*, 154, 109
- Gaia Collaboration. 2020, *VizieR Online Data Catalog*, I/350
- Gaia Collaboration, Brown, A. G. A., Vallenari, A., et al. 2021, *A&A*, 649, A1
- Gänsicke, B. T., Schreiber, M. R., Toloza, O., et al. 2019, *Nature*, 576, 61
- Gauba, G. & Parthasarathy, M. 2004, *A&A*, 417, 201
- Gauba, G., Parthasarathy, M., Kumar, B., Yadav, R. K. S., & Sagar, R. 2003, *A&A*, 404, 305
- Gehr, R. D., Marchetti, J., McMillan, S., et al. 2020, *The Astronomer's Telegram*, 13518, 1
- Ginzburg, S., Schlichting, H. E., & Sari, R. 2018, *MNRAS*, 476, 759
- Gonzalez, D. & Reisenegger, A. 2010, *A&A*, 522, A16
- Goudfrooij, P., Girardi, L., & Correnti, M. 2017, *ApJ*, 846, 22

- Graczyk, D., Pietrzyński, G., Galan, C., et al. 2021, *A&A*, 649, A109
- Granzer, T., Schüssler, M., Caligari, P., & Strassmeier, K. G. 2000, *A&A*, 355, 1087
- Grinin, V. P., Kiselev, N. N., Minikulov, N. K., Chernova, G. P., & Voshchinnikov, N. V. 1991, *Ap&SS*, 186, 283
- Guillot, S., Kerr, M., Ray, P. S., et al. 2019, *ApJ*, 887, L27
- Guinan, E., Wasatonic, R., Calderwood, T., & Carona, D. 2020, *The Astronomer's Telegram*, 13512, 1
- Guinan, E. F. & Engle, S. G. 2007, arXiv e-prints, arXiv:0711.1530
- Guinan, E. F., Ribas, I., Fitzpatrick, E. L., et al. 2000, *ApJ*, 544, 409
- Guzik, J. A., Kaye, A. B., Bradley, P. A., Cox, A. N., & Neuforge, C. 2000, *ApJ*, 542, L57
- Guzik, J. A. & Roth, M. 2021, *Frontiers in Astronomy and Space Sciences*, 8, 97
- Gvaramadze, V. V., Kroupa, P., & Pflamm-Altenburg, J. 2010, *A&A*, 519, A33
- Gvaramadze, V. V., Pflamm-Altenburg, J., & Kroupa, P. 2011, *A&A*, 525, A17
- Haisch, B., Strong, K. T., & Rodono, M. 1991, *ARA&A*, 29, 275
- Hallakoun, N., Xu, S., Maoz, D., et al. 2017, *MNRAS*, 469, 3213
- Hallam, K. L. & Wolff, C. L. 1981, *ApJ*, 248, L73
- Harder, J. W., Fontenla, J. M., Pilewskie, P., Richard, E. C., & Woods, T. N. 2009, *Geophys. Res. Lett.*, 36, L07801
- Henry, G. W., Marcy, G. W., Butler, R. P., & Vogt, S. S. 2000, *ApJ*, 529, L41
- Hobbs, G., Lyne, A. G., Kramer, M., Martin, C. E., & Jordan, C. 2004, *MNRAS*, 353, 1311
- Høg, E., Fabricius, C., Makarov, V. V., et al. 2000, *A&A*, 355, L27
- Holman, M. J., Fabrycky, D. C., Ragozzine, D., et al. 2010, *Science*, 330, 51
- Horvat, M., Conroy, K. E., Jones, D., & Prša, A. 2019, *ApJS*, 240, 36
- Howard, A. W., Marcy, G. W., Bryson, S. T., et al. 2012, *ApJS*, 201, 15
- Humphreys, R. M., Davidson, K., Richards, A. M. S., et al. 2021, *AJ*, 161, 98
- Humphreys, R. M. & Jones, T. J. 2022, *AJ*, 163, 103
- Hutsemekers, D. 1985, *A&AS*, 60, 373
- Íñiguez-Pascual, D., Viganò, D., & Torres, D. F. 2022, *MNRAS*, 516, 2475
- Iglesias, C. A., Rogers, F. J., & Wilson, B. G. 1992, *ApJ*, 397, 717
- Ignace, R., Fullard, A., Shrestha, M., et al. 2022, *ApJ*, 933, 5
- Irwin, J. M., Quinn, S. N., Berta, Z. K., et al. 2011, *ApJ*, 742, 123
- Ivanova, N., Justham, S., Chen, X., et al. 2013, *A&A Rev.*, 21, 59
- Jadhav, V. V. & Subramaniam, A. 2021, *MNRAS*, 507, 1699
- Jadlovský, D., Krtička, J., Paunzen, E., & Štefl, V. 2023, *New A*, 99, 101962
- Jenniskens, P. & Greenberg, J. M. 1993, *A&A*, 274, 439
- Johnson, H. R. & Luttermoser, D. G. 1987, *ApJ*, 314, 329
- Kaluzny, J. & Rucinski, S. M. 2003, *AJ*, 126, 237
- Kenworthy, M. A. & Mamajek, E. E. 2015, *ApJ*, 800, 126
- Khokhlov, S. A., Miroshnichenko, A. S., Zharikov, S. V., et al. 2018, *ApJ*, 856, 158
- Kloppenborg, B., Stencel, R., Monnier, J. D., et al. 2010, *Nature*, 464, 870
- Knigge, C., Baraffe, I., & Patterson, J. 2011, *ApJS*, 194, 28
- Kobulnicky, H. A., Chick, W. T., Schurhammer, D. P., et al. 2016, *ApJS*, 227, 18
- Kochukhov, O. & Ryabchikova, T. A. 2018, *MNRAS*, 474, 2787
- Konacki, M., Torres, G., Jha, S., & Sasselov, D. D. 2003, *Nature*, 421, 507
- Köpp, F., Horvath, J. E., Hadjimichef, D., Vasconcellos, C. A. Z., & Hess, P. O. 2023, *International Journal of Modern Physics D*, 32, 2350046
- Korčáková, D. 2022, *FS CMA stars: History, Properties, and Challenges*, habilitation thesis, Faculty of Mathematics and Physics, Charles University, Prague

- Korčáková, D., Miroshnichenko, A. S., Zharikov, S. V., et al. 2020, *Mem. Soc. Astron. Italiana*, 91, 118
- Korčáková, D., Sestito, F., Manset, N., et al. 2022, *A&A*, 659, A35
- Korčáková, D., Shore, S. N., Miroshnichenko, A., et al. 2019, in *Astronomical Society of the Pacific Conference Series*, Vol. 519, *Radiative Signatures from the Cosmos*, ed. K. Werner, C. Stehle, T. Rauch, & T. Lanz, 155
- Kowalski, A. F. & Allred, J. C. 2018, *ApJ*, 852, 61
- Krtićka, J. & Feldmeier, A. 2018, *A&A*, 617, A121
- Krtićka, J., Mikulášek, Z., Henry, G. W., et al. 2019, *A&A*, 625, A34
- Krtićka, J., Mikulášek, Z., Kurfürst, P., & Oksala, M. E. 2022, *A&A*, 659, A37
- Krtićka, J., Mikulášek, Z., Zverko, J., & Prvák, M. 2014, in *Putting A Stars into Context: Evolution, Environment, and Related Stars*, ed. G. Mathys, E. R. Griffin, O. Kochukhov, R. Monier, & G. M. Wahlgren, 205–213
- Krtićková, I. & Krtićka, J. 2018, *MNRAS*, 477, 236
- Kurtz, D. W. 1990, *ARA&A*, 28, 607
- Kučerová, B., Korčáková, D., Polster, J., et al. 2013, *A&A*, 554, A143
- Labadie-Bartz, J., Pepper, J., McSwain, M. V., et al. 2017, *AJ*, 153, 252
- Ladjal, D., Barlow, M. J., Groenewegen, M. A. T., et al. 2010, *A&A*, 518, L141
- Lagrange, A. M., Rubini, P., Nowak, M., et al. 2020, *A&A*, 642, A18
- Lamers, H. J. G. L. M., Zickgraf, F.-J., de Winter, D., Houziaux, L., & Zorec, J. 1998, *A&A*, 340, 117
- Lanz, T., Artru, M. C., Le Dourneuf, M., & Hubeny, I. 1996, *A&A*, 309, 218
- Larson, K. A. & Whittet, D. C. B. 2005, *ApJ*, 623, 897
- Lata, S., Pandey, A. K., Sagar, R., & Mohan, V. 2002, *A&A*, 388, 158
- Lavie, B., Ehrenreich, D., Bourrier, V., et al. 2017, *A&A*, 605, L7
- Legnardi, M. V., Milone, A. P., Cordini, G., et al. 2023, *MNRAS*, 522, 367
- Levesque, E. M. & Massey, P. 2020, *ApJ*, 891, L37
- Li, A. & Draine, B. T. 2001, *ApJ*, 554, 778
- Lim, B., Rauw, G., Nazé, Y., et al. 2019, *Nature Astronomy*, 3, 76
- Lopez, E. D., Fortney, J. J., & Miller, N. 2012, *ApJ*, 761, 59
- Lorimer, D. R. & Kramer, M. 2004, *Handbook of Pulsar Astronomy*, Vol. 4
- Loukaidou, G. A., Gazeas, K. D., Palafouta, S., et al. 2022, *MNRAS*, 514, 5528
- Ludendorff, H. 1903, *Astronomische Nachrichten*, 164, 81
- Luna, G. J. M., Sokoloski, J. L., Mukai, K., & Nelson, T. 2013, *A&A*, 559, A6
- Manser, C. J., Gänsicke, B. T., Eggl, S., et al. 2019, *Science*, 364, 66
- Martin, D. C., Seibert, M., Neill, J. D., et al. 2007, *Nature*, 448, 780
- Mayor, M. & Queloz, D. 1995, *Nature*, 378, 355
- Merc, J., Beck, P. G., Mathur, S., & García, R. A. 2023, *arXiv e-prints*, arXiv:2312.16126
- Merc, J., Gális, R., & Wolf, M. 2019, *Research Notes of the American Astronomical Society*, 3, 28
- Michaud, G., Richer, J., & Richard, O. 2011, *A&A*, 529, A60
- Miglio, A., Chiappini, C., Morel, T., et al. 2013, *MNRAS*, 429, 423
- Mignani, R. P. 2011, *Advances in Space Research*, 47, 1281
- Mikołajewska, J. 2012, *Baltic Astronomy*, 21, 5
- Mikulášek, Z., Krtićka, J., Henry, G. W., et al. 2011, *A&A*, 534, L5
- Mikulášek, Z., Krtićka, J., Shultz, M. E., et al. 2020, in *Stellar Magnetism: A Workshop in Honour of the Career and Contributions of John D. Landstreet*, ed. G. Wade, E. Alecian, D. Bohlender, & A. Sigut, Vol. 11, 46–53
- Miroshnichenko, A. S. 2007, *ApJ*, 667, 497

- Miroshnichenko, A. S. 2017, in *Astronomical Society of the Pacific Conference Series*, Vol. 508, *The B[e] Phenomenon: Forty Years of Studies*, ed. A. Miroshnichenko, S. Zharikov, D. Korčáková, & M. Wolf, 285
- Miroshnichenko, A. S., Danford, S., Zharikov, S. V., et al. 2020, *ApJ*, 897, 48
- Miroshnichenko, A. S., Gray, R. O., Vieira, S. L. A., Kuratov, K. S., & Bergner, Y. K. 1999, *A&A*, 347, 137
- Miroshnichenko, A. S., Levato, H., Bjorkman, K. S., & Grosso, M. 2001, *A&A*, 371, 600
- Moe, M. & Di Stefano, R. 2017, *ApJS*, 230, 15
- Montargès, M., Cannon, E., Lagadec, E., et al. 2021, in *SF2A-2021: Proceedings of the Annual meeting of the French Society of Astronomy and Astrophysics*, ed. A. Siebert, K. Baillié, E. Lagadec, N. Lagarde, J. Malzac, J. B. Marquette, M. N'Diaye, J. Richard, & O. Venot, 13–18
- Montesinos, B. 1998, in *ESA Special Publication*, Vol. 413, *Ultraviolet Astrophysics Beyond the IUE Final Archive*, ed. W. Wamsteker, R. Gonzalez Riestra, & B. Harris, 91
- Morales-Calderón, M., Stauffer, J. R., Hillenbrand, L. A., et al. 2011, *ApJ*, 733, 50
- Moranchel-Basurto, A., Korčáková, D., & Chametla, R. O. 2023, *MNRAS*, 523, 5554
- Mukai, K., Luna, G. J. M., Cusumano, G., et al. 2016, *MNRAS*, 461, L1
- Munari, U. 2019, *The Impact of Binary Stars on Stellar Evolution*, 54, 77
- Munari, U., Traven, G., Masetti, N., et al. 2021, *MNRAS*, 505, 6121
- Neslušan, L. & Budaj, J. 2017, *A&A*, 600, A86
- Nutzman, P. A., Fabrycky, D. C., & Fortney, J. J. 2011, *ApJ*, 740, L10
- Oksala, M. E., Kochukhov, O., Krtička, J., et al. 2015, *MNRAS*, 451, 2015
- Oshagh, M., Boisse, I., Boué, G., et al. 2013, *A&A*, 549, A35
- Paczynski, B. 1976, in *Structure and Evolution of Close Binary Systems*, ed. P. Eggleton, S. Mitton, & J. Whelan, Vol. 73, 75
- Paczynski, B. & Sienkiewicz, R. 1984, *ApJ*, 286, 332
- Pál, A. 2008, *MNRAS*, 390, 281
- Pala, A. F., Gänsicke, B. T., Townsley, D., et al. 2017, *MNRAS*, 466, 2855
- Paquette, C., Pelletier, C., Fontaine, G., & Michaud, G. 1986, *ApJS*, 61, 197
- Pavlovski, K., Harmanec, P., Božić, H., et al. 1997, *A&AS*, 125, 75
- Perez-Becker, D. & Chiang, E. 2013, *MNRAS*, 433, 2294
- Peterson, D. M. 1970, *ApJ*, 161, 685
- Pétri, J. 2015, *A&A*, 574, A51
- Petroff, E., Hessels, J. W. T., & Lorimer, D. R. 2022, *The Astronomy and Astrophysics Review*, 30, 2
- Piecka, M. & Paunzen, E. 2021, *arXiv e-prints*, arXiv:2107.07230
- Pigulski, A., Baran, A., Bzowski, M., et al. 2019, *Science case for UVSat space mission*, https://uvsat.camk.edu.pl/files/UVSAT_Opracownai_Photo.pdf
- Piro, A. L. & Vissapragada, S. 2020, *AJ*, 159, 131
- Podsiadlowski, P., Rappaport, S., & Pfahl, E. D. 2002, *ApJ*, 565, 1107
- Porter, A., Grant, D., Blundell, K., & Lee, S. 2021, *MNRAS*, 501, 5554
- Pribulla, T., Chochol, D., Heckert, P. A., et al. 2001, *A&A*, 371, 997
- Pribulla, T., Chochol, D., Milano, L., et al. 2000, *A&A*, 362, 169
- Prvák, M., Liška, J., Krtička, J., Mikulášek, Z., & Lüftinger, T. 2015, *A&A*, 584, A17
- Rappaport, S., Levine, A., Chiang, E., et al. 2012, *ApJ*, 752, 1
- Rauer, H., Catala, C., Aerts, C., et al. 2014, *Experimental Astronomy*, 38, 249
- Reindl, N., Bainbridge, M., Przybilla, N., et al. 2019, *MNRAS*, 482, L93
- Ribas, I., Guinan, E. F., Güdel, M., & Audard, M. 2005, *ApJ*, 622, 680

- Ricker, G. R., Winn, J. N., Vanderspek, R., et al. 2015, *Journal of Astronomical Telescopes, Instruments, and Systems*, 1, 014003
- Ricker, G. R., Winn, J. N., Vanderspek, R., et al. 2014, in *Society of Photo-Optical Instrumentation Engineers (SPIE) Conference Series*, Vol. 9143, *Space Telescopes and Instrumentation 2014: Optical, Infrared, and Millimeter Wave*, ed. J. Oschmann, Jacobus M., M. Clampin, G. G. Fazio, & H. A. MacEwen, 914320
- Riley, T. E., Watts, A. L., Bogdanov, S., et al. 2019, *ApJ*, 887, L21
- Rivinius, T., Carciofi, A. C., & Martayan, C. 2013, *A&A Rev.*, 21, 69
- Ruciński, S. M. 1969, *Acta Astron.*, 19, 245
- Salmon, S. J. A. J., Eggenberger, P., Montalbán, J., et al. 2022, *A&A*, 659, A142
- Sanchis-Ojeda, R., Rappaport, S., Pallè, E., et al. 2015, *ApJ*, 812, 112
- Sanchis-Ojeda, R., Rappaport, S., Winn, J. N., et al. 2014, *ApJ*, 787, 47
- Schmidtobreick, L. 2013, *Central European Astrophysical Bulletin*, 37, 361
- Schneider, F. R. N., Ohlmann, S. T., Podsiadlowski, P., et al. 2020, *MNRAS*, 495, 2796
- Seager, S. & Mallén-Ornelas, G. 2003, *ApJ*, 585, 1038
- Seli, B., Vida, K., Moór, A., Pál, A., & Oláh, K. 2021, *A&A*, 650, A138
- Selvelli, P. & Gilmozzi, R. 2013, *A&A*, 560, A49
- Serenelli, A., Weiss, A., Aerts, C., et al. 2021, *A&A Rev.*, 29, 4
- Sheikina, T. A., Miroshnichenko, A. S., & Corporon, P. 2000, in *Astronomical Society of the Pacific Conference Series*, Vol. 214, *IAU Colloq. 175: The Be Phenomenon in Early-Type Stars*, ed. M. A. Smith, H. F. Henrichs, & J. Fabregat, 494
- Shore, S. N. 1990, *IAU Circ.*, 5005, 1
- Shvartzvald, Y., Waxman, E., Gal-Yam, A., et al. 2023, *arXiv e-prints*, arXiv:2304.14482
- Siegel, M. H., LaPorte, S. J., Porterfield, B. L., Hagen, L. M. Z., & Gronwall, C. A. 2019, *AJ*, 158, 35
- Smith, G. H. & Cochrane, K. M. 2020, *Ap&SS*, 365, 95
- Smith, M. A. 2001, *ApJ*, 562, 998
- Smith, N. 2014, *ARA&A*, 52, 487
- Southworth, J. 2015, in *Astronomical Society of the Pacific Conference Series*, Vol. 496, *Living Together: Planets, Host Stars and Binaries*, ed. S. M. Rucinski, G. Torres, & M. Zejda, 164
- Southworth, J., Maxted, P. F. L., & Smalley, B. 2005, *A&A*, 429, 645
- Stecher, T. P. 1965, *ApJ*, 142, 1683
- Stencel, R. E., Carpenter, K. G., & Hagen, W. 1986, *ApJ*, 308, 859
- Sun, M., Jiang, B., Zhao, H., & Ren, Y. 2021, *ApJS*, 256, 46
- Sundqvist, J. O., Puls, J., & Feldmeier, A. 2010, *A&A*, 510, A11
- Šurlan, B., Hamann, W.-R., Aret, A., et al. 2013, *A&A*, 559, A130
- Szabó, G. M., Pál, A., Derekas, A., et al. 2012, *MNRAS*, 421, L122
- Tafoya, D., Gómez, Y., & Rodríguez, L. F. 2004, *ApJ*, 610, 827
- Takata, J. & Cheng, K. S. 2017, *ApJ*, 834, 4
- Torres, G., Andersen, J., & Giménez, A. 2010, *A&A Rev.*, 18, 67
- Turner, D. G. 1979, *PASP*, 91, 642
- van Buren, D. & McCray, R. 1988, *ApJ*, 329, L93
- Van Eylen, V., Agentoft, C., Lundkvist, M. S., et al. 2018, *MNRAS*, 479, 4786
- Vanderbosch, Z., Hermes, J. J., Dennihy, E., et al. 2020, *ApJ*, 897, 171
- Vanderburg, A., Johnson, J. A., Rappaport, S., et al. 2015, *Nature*, 526, 546
- Vanderburg, A., Rappaport, S. A., Xu, S., et al. 2020, *Nature*, 585, 363
- Varga, J., Gerják, T., Ábrahám, P., et al. 2019, *MNRAS*, 485, 3112

- Vida, K., Oláh, K., Kóvári, Z., et al. 2019, *ApJ*, 884, 160
- Vidotto, A. A. 2020, in *Solar and Stellar Magnetic Fields: Origins and Manifestations*, ed. A. Kosovichev, S. Strassmeier, & M. Jardine, Vol. 354, 259–267
- Vučković, M., Østensen, R. H., Németh, P., Bloemen, S., & Pápics, P. I. 2016, *A&A*, 586, A146
- Walker, G., Matthews, J., Kuschnig, R., et al. 2003, *PASP*, 115, 1023
- Wang, B. & Han, Z. 2012, *New A Rev.*, 56, 122
- Weingartner, J. C. & Draine, B. T. 2001, *ApJ*, 548, 296
- Weiss, W. W., Rucinski, S. M., Moffat, A. F. J., et al. 2014, *PASP*, 126, 573
- Weiss, W. W., Zwintz, K., Kuschnig, R., et al. 2021, *Universe*, 7, 199
- Welsh, B. Y., Wheatley, J., Browne, S. E., et al. 2006, *A&A*, 458, 921
- Werner, N., Řípa, J., Thöne, C., et al. 2024, *Space Sci. Rev.*, 220, 11
- White, R. L. & Becker, R. H. 1985, in *Bulletin of the American Astronomical Society*, Vol. 17, 753
- Wilson, O. C. 1978, *ApJ*, 226, 379
- Wilson, R. E. 1971, *ApJ*, 170, 529
- Wilson, R. E. 1990, *ApJ*, 356, 613
- Wolszczan, A. & Frail, D. A. 1992, *Nature*, 355, 145
- Wu, Z., Ricigliano, G., Kashyap, R., Perego, A., & Radice, D. 2022, *MNRAS*, 512, 328
- Xiao, D., Wang, F., & Dai, Z. 2021, *Science China Physics, Mechanics & Astronomy*, 64, 249501
- Xu, S., Hallakoun, N., Gary, B., et al. 2019, *AJ*, 157, 255
- Xu, S., Jura, M., Dufour, P., & Zuckerman, B. 2016, *ApJ*, 816, L22
- Yao, G.-R., Huang, L., Yu, C., & Shen, Z.-Q. 2018, *ApJ*, 854, 10
- Zajaček, M., Czerny, B., Jaiswal, V. K., et al. 2023, arXiv e-prints, arXiv:2306.15082